A STUDY OF NONLINEAR CHARACTERISTICS OF MOSFETS USING CROSS MODULATION

by

MUKESH KUMAR

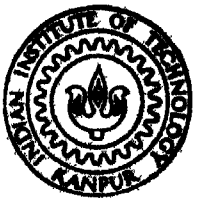

DEPARTMENT OF ELECTRICAL ENGINEERING

INDIAN INSTITUTE OF TECHNOLOGY, KANPUR

APRIL, 1987

A STUDY OF NONLINEAR CHARACTERISTICS OF MOSFETS USING CROSS MODULATION

A Thesis Submitted
In Partial Fulfilment of the Requirements
for the Degree of

MASTER OF TECHNOLOGY

by

MUKESH KUMAR

to the

DEPARTMENT OF ELECTRICAL ENGINEERING

INDIAN INSTITUTE OF TECHNOLOGY, KANPUR

APRIL 1987

CERTIFICATE

This is to certify that this work ''A STUDY OF NONLINEAR CHARACTERISTICS OF MOSFETS USING CROSS MODULATION'' by Mukesh Kumar has been carried out under my supervision and this has not been submitted elsewhere for a degree.

April, 1987.

(R. Sharan)
Professor
Department of Electrical Engineering
Indian Institute of Technology
KANPUR.

ACKNOWLEDGEMENT

It gives me great pleasure to place on record my deep sense of gratitude to Dr. R. Sharan for his inspiring guidance throughout the course of my work His novel ideas and concepts helped me in shaping my attitude towards the subject and carrying out this modest piece of work.

I am very much obliged to Dr. R. Raghuram and Dr. K.R. Srivathsan,and the other faculty members of the Department who enlightened me at many stages of the work through invaluable discussions.

I also take this opportunity to thank Mr. J. John for his generous cooperation.

I would like to extend my sincere gratitude to all of my friends, in particular, Sachi, Ashok, Narayan, Biswa and Subrata for their nice company.

Finally, Mr. L.S. Bajpai deserves credit for his excellent typing work.

Mukesh Kumar

ABSTRACT

Present MOSFET models used for CAD purposes, lack the level of precision required for proper analog circuit design. In the present work a nonlinear method, cross modulation is used to describe the behaviour of MOSFLT. It is claimed that this method can reveal subtle nuances of the behaviour of a device and its model. Experiments have been done to measure cross modulation in all the regions of operation. Cross modulation behaviour has also been simulated using SPICE. Comparison between the two is presented. It is shown that SPICE model is inadequate to describe the nonlinear characteristics of MOSFET. Emphasis is given on moderate inversion region for which no suitable simple model is presently available. Noise behaviour of MOSFET has also been measured in moderate inversion and strong inversion regions. It has been found that some correlation exists between the noise and the nonlinear behaviour of the device.

CONTENTS

LIST OF FIGURES

CHAPTER I

INTRODUCTION

Prior to the mid-1970s, MOS technology was utilized primarily for memory and logic function and the analog functions that were required in a given system were typically implemented by using bipolar integrated circuits. However, in the more recent years, the steady increase in chip complexity brought about by the continuing improvement in lithographic resolution have created the economic incentive to implement subsystems containing both analog and digital functions on a single integrated circuit. This trend is likely to continue, since most signals in need of processing are analog at the source, yet, the device models available are usually good enough only for digital MOS circuit design.

Another trend seen presently is the application of MOSFET in low-voltage and low power applications. The simulation of the behaviour in weak inversion region becomes important in these applications, because very often the MOS circuit needs to be operated in this region. MOSFET are said to have more noise as we go from strong inversion to weak inversion region [1].

The aim of our project was to investigate the precision modelling of devices, in weak inversion, moderate inversion and strong inversion regions. For this we have used cross modulation, a non linear effect to characterize the device.

Cross modulation is an undesired phenomenon in communication system and through suitable design technique attempt are made to eliminate it. In the present work, we take another view and explore those regions of operations where cross modulation is significant. The significance of the characterization of a device using cross modulation lies in the fact that it can reveal the fine details of the device characteristics very easily.

Many authors have made attempts to simulate the cross modulation behaviour of MOSFET using power series approach for low frequency behaviour [2,3] and Volterra series approach for high frequency behaviour [4]. Miharan [5] also developed a model using curve fitting approach to qualitatively describe the cross modulation behaviour. But these approaches are useful only for simulation of the non linear behaviour. No physical insight about the device characteristic is obtained from them.

General formulations for device behaviour have been developed. There exist single expressions, which are valid in all regions of operation. They restore the higher order terms of the device characteristic in a better way by avoiding the artificial transitions from one region to the next. But due to the high complexity of these models, the use of different equations for different region of operation is considered to be necessary. A general assumption that is made in popular CAD model is that weak and strong inversion regions expression are valid in adjacent regions. This seems too crude for analog

work. It has been suggested in our work that suitable approximations can be made in the general model to get an analytic expression in this region. The necessary parameters can be extracted by cross modulation measurement.

In the present work, we have probed all the regions of operation of MOSFETs using cross modulation technique. This technique is shown to be particularly useful for describing the behaviour of the device in moderate inversion region (a region between weak inversion and strong inversion region). The popular CAD models give large errors while describing the nonlinearities of device. This was verified using SPICE simulation.

Noise measurements have also been made is strong inversion and moderate inversion regions. It is shown that noise behaviour in the moderate inversion region can not be approximated by the strong inversion and weak inversion region characteristics. Proper modelling of noise in the moderate inversion region is emphasized. Some correlation is seen between the noise behaviour and nonlinear behaviour of the MOSFET.

The nonlinear behaviour of devices and cross modulation are described in Chapter II. The experimental part is also given in this chapter. In Chapter 3, we have tried to explain the results of cross modulation experiment. Modelling in moderate inversion is emphasized there. The experimental part

has been compared with the SPICE simulation. The experimental procedures for extraction of the necessary SPICE parameters are also described. Chapter 4 gives the experimentation part of noise measurement of MOSFET. The results are correlated with the cross modulation data. Lastly in Chapter 5 the overall work has been summarized and some suggestions for further extension of this work have been made.

CHAPTER II

CROSS MODULATION THEORY AND MEASUREMENTS

All physical components and devices are inherently nonlinear. The nonlinear considerations play an important role in the operation of communication and electronic circuits. Intermodulation, cross modulation, harmonic generation, desensitization, gain compression/expression, and spurious response are the major nonlinear effect [6]. These terms are described briefly in Appendix (A).

Our investigation is directed towards cross modulation in FETs although other nonlinear effects such as intermodulation (which is closely related) could have been used as a measure of nonlinearity [7].

In this chapter, first we give a general discussion on sinusoidal steady state response of weakly nonlinear systems. Then we briefly describe the role of frequency mixes for understanding the generation of various frequency components. Cross modulation, which arises due to some of those frequency mixes, is discussed later with our experimental work.

2.1 SINUSOIDAL STEADY STATE RESPONSE OF WEAKLY NONLINEAR SYSTEMS

Let us consider a weakly nonlinear circuit with input $x(t)$ and output $y(t)$. Based upon Volterra analysis, the

nonlinear transfer function models the circuit as shown in Fig. 2.1. This model consists of the parallel combination of N block with each block having, as a common input, the circuit excitation $x(t)$. The output of the n^{th} block is denoted by $y_n(t)$; $n = 1,2,.....N$. The total response is obtained by summing the outputs of the individual blocks so as to yield

$$y(t) = y_1(t) + y_2(t) + ... + y_N(t)$$

$$= \sum_{n=1}^{N} y_n(t) \qquad (2.1)$$

The n^{th} block, characterized by the n^{th}-order nonlinear transfer function $H_n(f_1,f_2,....f_n)$ is of n^{th} order in the sense that multiplication of the input $x(t)$ by a constant A results in multiplication of the output $y_n(t)$ by the constant A^n. Blocks above N^{th} order are not included in the model because it is assumed they contribute negligibly to the output.

To study the sinusoidal steady state of weakly nonlinear systems, let the input to the model shown in Fig. 2.1 be a sum of Q sinusoidal signals. The excitation can be expressed as

$$x(t) = \sum_{q=1}^{Q} |E_q| \cos (2\pi f_q t + \theta_q) = \frac{1}{2} \sum_{q=-Q}^{Q} E_q \exp(j2\pi f_q t)$$

$$\ldots\ldots \qquad (2.2)$$

where E_q is the complex voltage of the q^{th} tone.

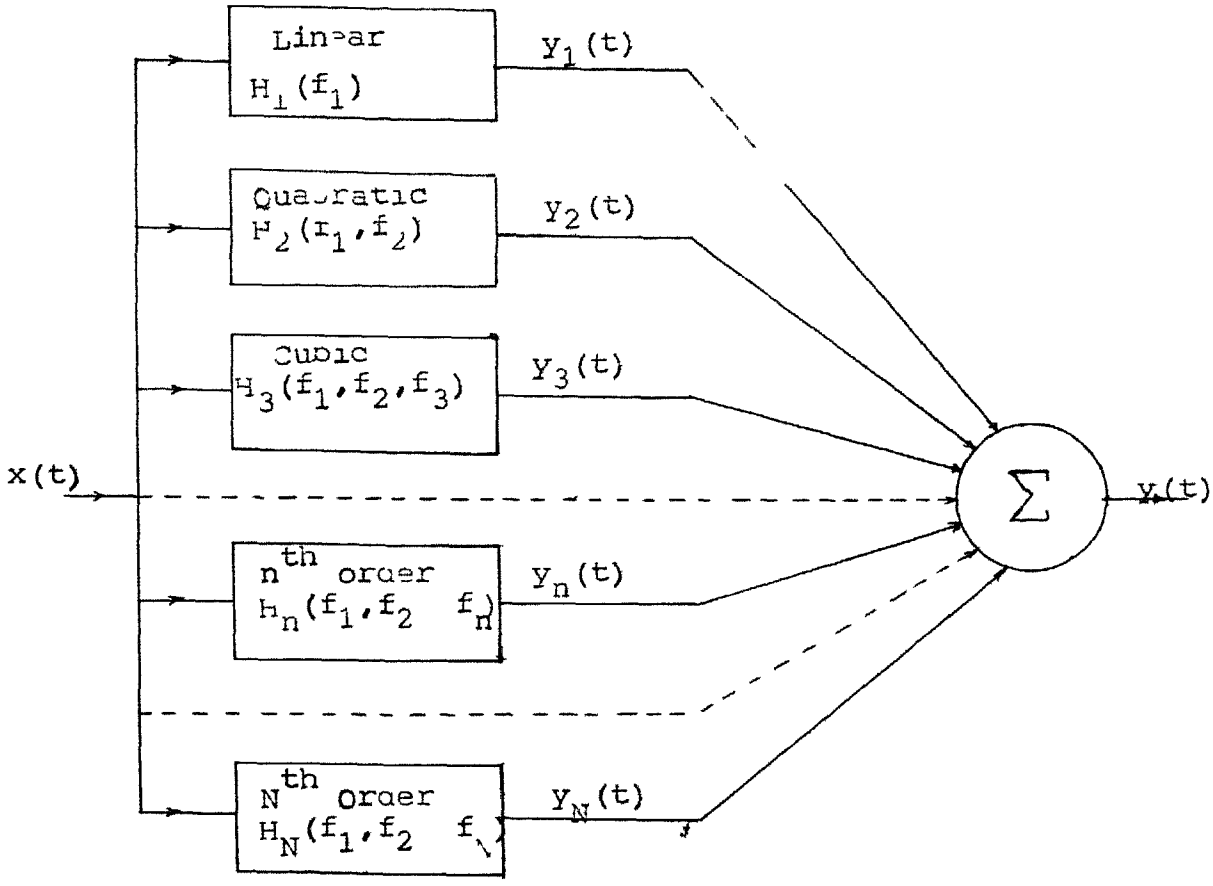

Fig 2 1 Model of a weakly nonlinear circuit

In the nonlinear transfer function approach the total response of the nonlinear system is expressed by (2.1), where [6]

$$y_n(t) = \frac{1}{2^n} \sum_{q_1=-Q}^{Q} \cdots \sum_{q_n=-Q}^{Q} E_{q_1} \cdots E_{q_n}$$

$$\times H_n(f_{q_1},\ldots\ldots,f_{q_n}) \exp[j2\pi(f_{q_1}+\ldots+f_{q_n})] \qquad (2.3)$$

This means that, when a sum of Q sinusoidal signals is applied to a nonlinear circuit, additional output frequencies are generated by the n^{th} order portion of the circuit consisting of all possible combinations of the input frequencies $-f_Q,\ldots\ldots,-f_1,f_1,\ldots\ldots,f_Q$ taken n at a time. As revealed in (2.3), $H_n(f_{q_1},\ldots\ldots,f_{q_n})$ is the nonlinear transfer function relating the output at frequency $(f_{q_1}+\ldots\ldots+f_{q_n})$ to the inputs at frequencies $f_{q_1}, f_{q_2},\ldots\ldots,f_{q_n}$.

2.2 ROLE OF FREQUENCY MIXES IN THE GENERATION OF VARIOUS FREQUENCY COMPONENTS

The process by which two or more signals combine in a nonlinear manner so as to produce new frequency components is known as intermodulation. In this broad sense, intermodulation encompasses all of the nonlinear effects mentioned at the beginning of this chapter. For the ease of distinction from other nonlinear effects we would give it a restrictive interpretation as followed in most of literature. Specifically,

intermodulation is used to refer to only those nonlinear frequency components, resulting from frequency mixes, that are not included in the catagories of cross modulation, harmonic generation, desensitization, gain compression/ expression and spurious response.

Let m_k denotes the number of times the frequency f_k appears in a particular frequency mix. Then for input $x(t)$ given by eq. (2.2) all the frequency mixes are represented by the frequency mix vector

$$\underline{m} = (m_{-Q}, \ldots\ldots m_{-1}, m_1, \ldots\ldots, m_Q) \tag{2.4}$$

The corresponding frequency is

$$f_m = \sum_{\substack{k=-Q \\ k \neq 0}}^{Q} m_k f_k \tag{2.5}$$

For an n^{th} order component of the response, the m_k's obey the constraint

$$\sum_{\substack{k=-Q \\ k \neq 0}}^{Q} m_k = m_{-Q} + \ldots\ldots + m_{-1} + m_1 + \ldots\ldots + m_Q = n \tag{2.6}$$

Therefore, the output frequencies in eq. (2.3) can be interpreted as those intermodulation frequencies that can be generated by all possible choices of the m_k's such that eq. (2.6) is satisfied.

Using eq. (2.3) it can be shown that for a particular vector $\underline{m}$, corresponding to n^{th} order, the output is given by [6]

$$y_n(t;\underline{m}) = \frac{(n;\underline{m})}{2^n} |E_1|^{(m_1+m_{-1})} \ldots\ldots |E_Q|^{(m_Q+m_{-Q})}$$

$$\cdot\ |H_n(\underline{m})|\ \cos\ [2\pi f_{\underline{m}} t + \theta_{\underline{m}} + \gamma_n(\underline{m})] \qquad (2.7)$$

where $$(n,\underline{m}) = \frac{n!}{m_{-Q}! \ldots\ldots m_{-1}!\ m_1!\ \ldots\ m_Q!} \qquad (2.8)$$

$$\theta_m = \sum_{\substack{k=-Q \\ k \neq 0}}^{Q} m_k\theta_k = (m_1 - m_{-1})\ \theta_1 + \ldots\ldots + (m_Q - m_{-Q})\theta_Q$$

$H_n(\underline{m})$ is n^{th} order nonlinear transfer function for the mix vector $\underline{m}$. It is represented as

$$H_n(\underline{m}) = |H_n(\underline{m})|\ \exp[j\gamma_n(\underline{m})]$$

$$= H_n(\underbrace{-f_Q,\ldots,-f_Q}_{m_Q},\ldots\ldots,\underbrace{f_{-1},\ldots,f_{-1}}_{m_{-1}},$$

$$\underbrace{f_1,\ldots,f_1}_{m_1},\ldots\ldots,\underbrace{f_Q,\ldots,f_Q}_{m_Q}) \qquad (2.9)$$

The n^{th} order portion y(t) can now be written as

$$y_n(t) = \sum_{\underline{m}} y_n(t;\underline{m}) \qquad (2.10)$$

where the summation over $\underline{m}$ is defined to be

$$\sum_{\underline{m}} = \sum_{m_{-Q}=0}^{n} \ldots\ldots \sum_{m_{-1}=0}^{n} \sum_{m_1=0} \ldots\ldots \sum_{m_Q=0}^{n} \qquad (2.11)$$

with the condition that eq. (2.6) is satisfied.

It can be shown that the summation in (2.10) for obtaining $y_n(t)$ extends over

$$M = \frac{(2Q + n - 1)!}{n!\,(2Q - 1)!} \tag{2.12}$$

distinct vector $\underline{m}$.

2.3 CROSS MODULATION

Cross modulation is the nonlinear effect whereby modulation from one signal is transfered to another Thus, if two sinusoidal signals only one of which is amplitude modulated, are applied to a nonlinear device or circuit, then at the output one finds that that signal, which at the input was not modulated, also gets some modulation. This process is well known in communication systems and because of its understable effects, efforts are made to eliminate through suitable device and circuit design [8].

The basic process of cross modulation can be further explained with the help of schematic diagram shown in Fig. 2.2. Here a sinusoidal signal $x_s(t)$ of frequency f_s and an unmodulated signal $x_I(t)$ of frequency f_I and sidebands $f_I \pm f_m$ are summed and applied as input $x(t)$ to a nonlinear system (which is our case is a MOSFET amplifier). A pictorial representation of the input voltage $x(t)$, as would be seen on spectrum analyzer, is shown in Fig. 2.3(a).

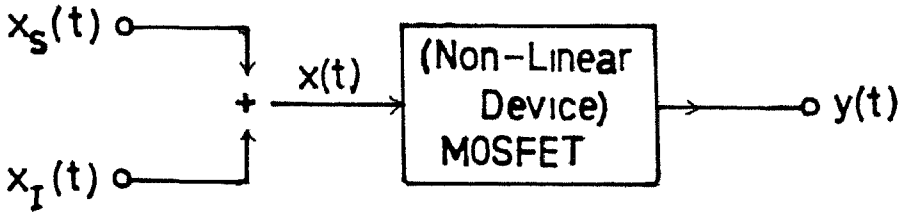

Fig 2 2 Schematic diagram for cross modulation

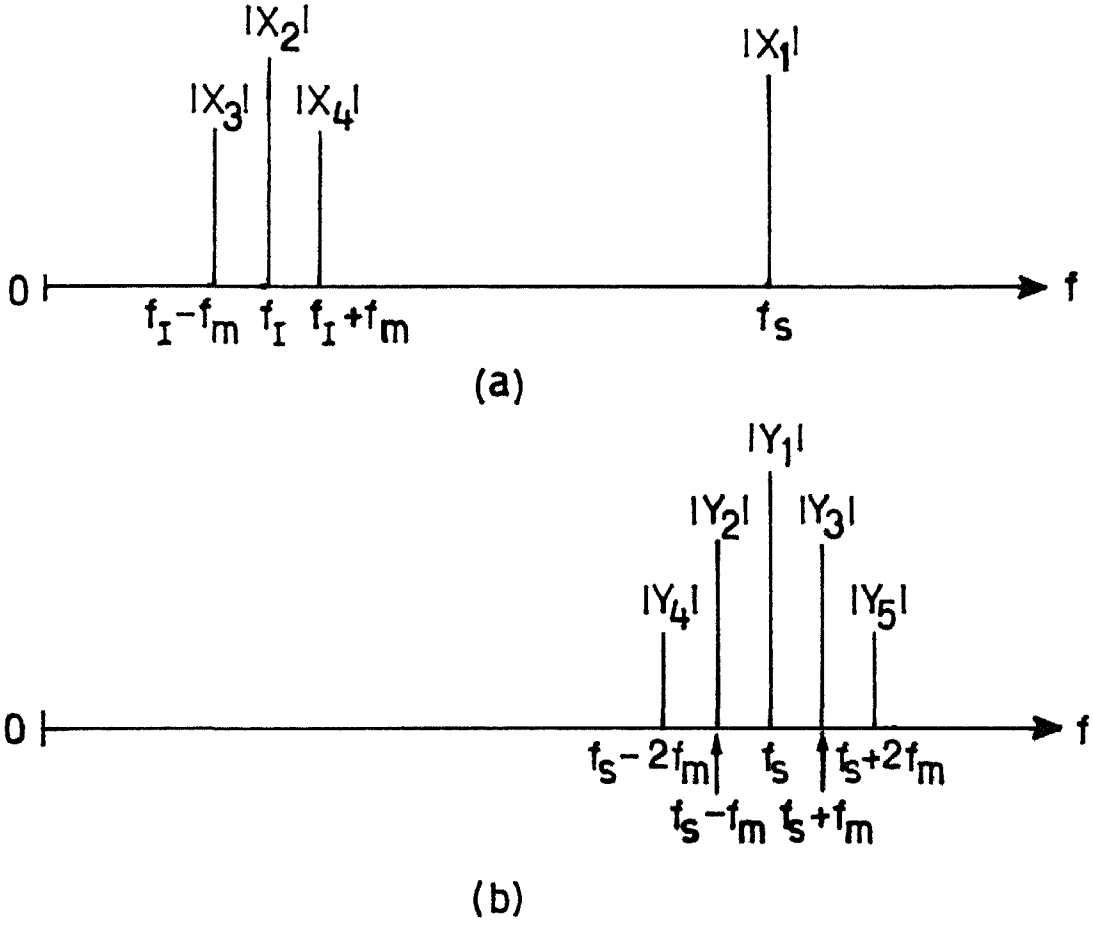

Fig 2 3 (a) Input signal spectrum

(b) Output signal spectrum in the vicinity of f_s

In response to the input x(t) there are many different terms contained in the output as can be seen from eq. (2.12) In the present work we concentrate only on the output signals at f_s and $f_s \pm f_m$, which alongwith the signals at $f_s \pm 2f_m$ are shown in Fig. 2.3(b).

Let $\bar{X}_1$, $\bar{X}_2$, $\bar{X}_3$ and $\bar{X}_4$ denote the voltage phasor in the input signal at frequencies $f_1 = f_s$, $f_2 = f_I$, $f_3 = f_I - f_m$ and $f_4 = f_I + f_m$ respectively, and the voltage phasors in the output at frequencies f_s, $f_s - f_m$, $f_s + f_m$, $f_s - 2f_m$ and $f_s + 2f_m$ be denoted by $\bar{Y}_1$, $\bar{Y}_2$, $\bar{Y}_3$, $\bar{Y}_4$ and $\bar{Y}_5$ respectively. The modulation index is denoted by m_I, where

$$m_I = \frac{(\bar{X}_3 + \bar{X}_4)}{(\bar{X}_2)} \tag{2.13}$$

The frequency mixes of our interest (which contribute to cross modulation) are tabulated in Table 2.1. Because the excitation consists of 4 input frequencies by eq. (2.4) $\underline{m} = (m_{-4}, m_{-3}, m_{-2}, m_{-1}, m_1, m_2, m_3, m_4)$. We have neglected the contribution due to the nonlinear effects above fourth order. To each vector $\underline{m}$ there is a vector $\underline{m}'$ also that yields the -ve frequency. The positive and negative frequency terms combine to produce real sinusoidal components.

Now, we can use eq. (2.7) to find out the output due to each of these frequency mixes and then find out the expressions for $|Y_1|$ and $|Y_2|$ as

$$|Y_1| = K_1 |\bar{X}_1| + 3/2 K_3 |\bar{X}_1| |\bar{X}_2|^2 \left[1 + \frac{m_I^2}{2} + \frac{1}{2}\left|\frac{\bar{X}_1}{\bar{X}_2}\right|^2\right] \tag{2.14}$$

TABLE 2.1. Frequency Mixes of Interest in the Cross Modulation Analysis.

$m=(m_{-4},m_{-3},m_{-2},m_{-1},m_1,m_2,m_3,m_4)$								
m_{-4}	m_{-3}	m_{-2}	m_{-1}	m_1	m_2	m_3	m_4	f_m
0	0	0	0	1	0	0	0	$f_1 = f_s$
1	0	0	0	1	0	0	1	$-f_4+f_1+f_4 = f_1 = f_s$
0	1	0	0	1	0	1	0	$-f_3+f_1+f_3 = f_1 = f_s$
0	0	1	0	1	1	0	0	$-f_2+f_1+f_2 = f_1 = f_s$
0	0	0	1	2	0	0	0	$-f_1+2f_1 = f_1 = f_s$
1	0	0	0	1	1	0	0	$-f_4+f_1+f_2 = f_s - f_m$
0	0	1	0	1	0	1	0	$-f_2+f_1+f_3 = f_s - f_m$
0	0	1	0	1	0	0	1	$-f_2+f_1+f_4 = f_s + f_m$
0	1	0	0	1	1	0	0	$-f_3+f_1+f_2 = f_s + f_m$
1	0	0	0	1	0	1	0	$-f_4+f_1+f_3 = f_s - 2f_m$
0	1	0	0	1	0	0	1	$-f_3+f_1+f_4 = f_s + 2f_m$

$$|\bar{Y}_2| = |\bar{Y}_3| = \tfrac{3}{2} \cdot K_3 |\bar{X}_1| |\bar{X}_2|^2 m_I \qquad (2.15)$$

Here, we have assumed the third order transfer function equal to a constant K_3 over the frequency range of interest. The first order transfer function is denoted by K_1.

Cross modulation ratio is defined as

$$\text{CMR} = \frac{\text{(peak to peak variation in envelope of desired signal due to sidebands at } f_s \pm f_m)}{\text{(amplitude of desired carriers with interferer removed)}} \qquad (2.16)$$

Using eq. (2.14) and (2.15)

$$CMR = \frac{6 K_3 |X_2|^2 m_I}{K_1 + 3/4 . K_3 |X_1|^2} \qquad (2.17)$$

The second term in the demominator of (2.17) is usually negligible with respect to the first. The cross modulation ratio is then approximated by

$$CMR \approx 6 \frac{K_3}{K_1} |X_1|^2 m_I \qquad (2.18)$$

Thus we see that CMR can be used as an indicator of the amount of nonlinearity present in a device. This gives the ratio of undesired component to the desired one. We can also see the nonlinear behaviour of device as a function of bias variation.

The third order transfer function of the device can be found using eq. (2.15) because all other quantities are experimentally measurable

2.4 MEASURMENT OF CROSS MODULATION IN MOSFET

2.4.1 Description of set-up

The cross modulation measurements have been made on an n-channel enhancement MOSFET in the CMOS inverter chip CD4007. It has three inverters of which one is internally connected and the remaining two NMOS and PMOS pairs are left without interconnection.

The block diagram of the cross modulation experiment (as given in Fig. 2.2) has already been described. Circuit diagram of a set up is shown in Fig. 2.4. The unmodulated signal is taken from test oscillator (H.P. model 651A) Modulating signal taken from another similar test oscillator, is fed to a function generator (Kikusui Model 4502) to get amplitude modulated output.

These two signals are then summed using op-amp summer Care was taken to avoid any nonlinear effect due to the summer itself. Use of 741 op-amp gave some cross modulation at its output due to its slew rate limitation. So we shifted over to the use of JFFT input op-amp CA 081, which has high slew rate.

Biasing arrangement of the MOSFET was made using two other op-amps. One of them acts as I-to-V converter for measurement of drain current I_D. Here again we need JFFT input op-amp for measurement of low drain currents and also for distortionless I to V converters. Drain and gate biases of the MOSFET are controlled using two ten-turn helipots, because we need precise variations of the voltages. Op-amp was used for drain bias to avoid any loading effect. The two capacitors in the gate circuit are used to reduce the effects of power supply ripples and noise.

V_{DS} and V_{GS} of the MOSFET are measured using HIL digital multimeter. The spectrum of the output signal V_o is seen on

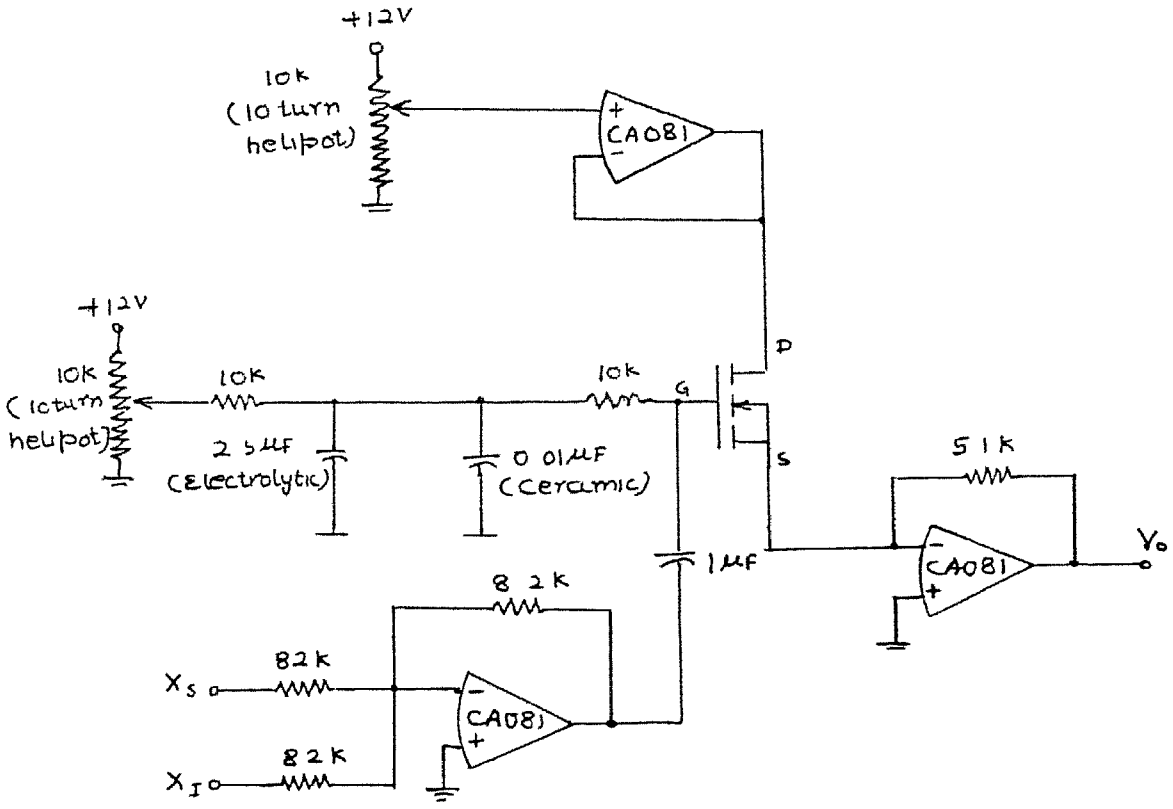

Fig 2 4 Circuit diagram for cross modulation measurement

a spectrum Analyzer (Takeda-Riken Model TR 4120). The settings of the spectrum analyzer were also very crucial for our measurements. The spectrum analyzer adds some nonlinearity to the signal before display on the screen. To minimize this, the signal to the spectrum analyzer is attenuated using a knob on the instrument itself, but if we attenuate the input signal too much then noise starts appearing on the screen. So a compromize was made throughout the experimentation so as to get nearly true spectrum on the screen of the spectrum analyzer.

2.4.2 Experimention

As mentioned in the last section, we get many different components at output of a nonlinear system in response to the input x(t). So we get many spectral lines on spectrum analyzer corresponding to these frequency components. The frequencies of input signal components are choosen so that we do not get any other intermodulation component at the frequencies corresponding to Y_2 and Y_3. The frequency of the unmodulated sinusoidal signal $X_s(t)$ is thus set at 52 KHz and that of the carrier of the modulated signal $X_I(t)$ at 14 KHz. The sinusoidal modulating signal of $X_I(t)$ is set at 1.5 KHz.

The following checks were performed on cross modulation before going for actual measurements :-

(a) A feature of eq. (2.14) and (2.15), is that if $|\bar{X}_1|$ and $|\bar{X}_2|$ are multiplied by an arbitrary factor C, with m_I kept constant, i.e. with $|\bar{X}_3|$ also multiplied by C, then the output $|Y_2|$ would

be multiplied by C^3 if the value of K_3 is truely a constant independent of input. This feature was verified experimentally. The observations on different changes in the inputs are given in Table 2.2.

TABLE 2.2. Dependance of Cross Modulation Components on Input Signal.

No.	INPUTS			OUTPUTS			
	$\lvert\bar{X}_1\rvert$	$\lvert\bar{X}_2\rvert$	$\lvert\bar{X}_3\rvert = \lvert\bar{X}_4\rvert$	$\lvert\bar{Y}_1\rvert$ with $\lvert\bar{X}_I\rvert$	$\lvert\bar{Y}_1\rvert$ without $\lvert\bar{X}_I\rvert$	$\lvert\bar{Y}_2\rvert = \lvert\bar{Y}_3\rvert$	$\lvert\bar{Y}_4\rvert = \lvert\bar{Y}_5\rvert$
1.	-28 dB	-22 db	-12db	-42 db	-45 db	-59 db	-79 db
2.	-30 db	-22 db	-12db	-44 db	-47 db	-61 db	-81 db
3.	-30 db	-24 db	-14db	-44 db	-47 db	-64 db	-85 db

(b) At the input, if the carrier at f_I is suppressed, there are only three components of input at f_s and $(f_I \pm f_m)$ Then at the output the spectra at $f_s \pm f_m$ get suppressed but those at $f_s \pm 2f_m$ continue to be present. The suppression of the spectra at $f_s \pm f_m$ is predicted by eq.(2.15) because if $|\bar{X}_2| = 0$ then $|\bar{Y}_2| = |\bar{Y}_3| = 0$. It can be shown [1] that amplitudes of spectra at $f_s \pm 2f_m$ are not dependant on $|\bar{X}_2|$ hence it is expected that they will not get affected if the carrier at f_I is suppressed.

(c) Variation of f_c, f_m and f_s should not a fect the cross modulation components.

After making the above mentioned checks, we measured cross modulation at different bias points in all the three

cross modulation at different bias points in all the three regions of operation of MOSFETs viz. weak inversion, strong inversion and linear region.

Cross modulation was first measured for variations of V_{GS}, while keeping V_{DS} constant. Cross modulation ratio (CMR) V/S V_{GS} is plotted in Fig. 2.5 on semi-log scale for V_{DS} = 0.25 V, 0.50 V and 1.0 V. The shape of the curve thus obtained agrees with the earlier results [2] as reported in literature.

We got some peaks in above plots in the linear region of MOSFET. So, to see them from another angle, we also measured cross modulation for variations of V_{DS}, while keeping V_{GS} constant. Plots of CMR V/S V_{DS} are shown in Fig. 2.6 for different V_{GS} values.

For low value of V_{GS}, CMR saturates at high values due to the nonlinearity of spectrum analyzer, so those curves can be disregarded. For higher values of V_{GS}, as V_{DS} is increased CMR rises first and then starts decreasing in the linear region itself. The peaks are more pronounced for low value of V_{GS}. This behaviour shows some source of nonlinearity in linear region, the effect of which decreases when V_{GS} is increased.

2.5 CONCLUSION

We began this chapter with the discussion on a general view of the behaviour of nonlinear circuits. This was necessary for understanding of the cross modulation behaviour. Cross modulation ratio was used as an index of nonlinearity present in

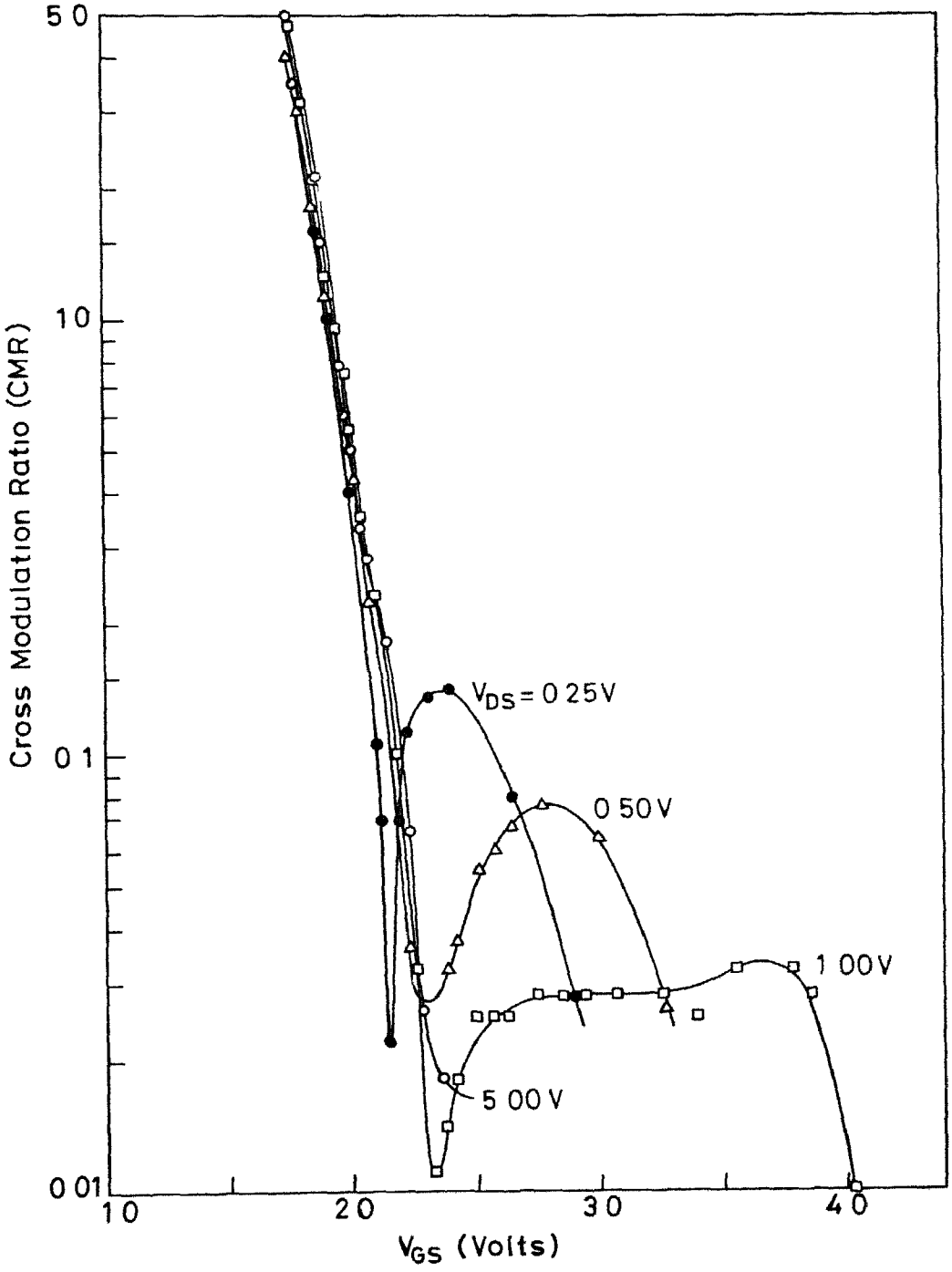

Fig 2 5 Cross modulation characteristic versus V_{GS}

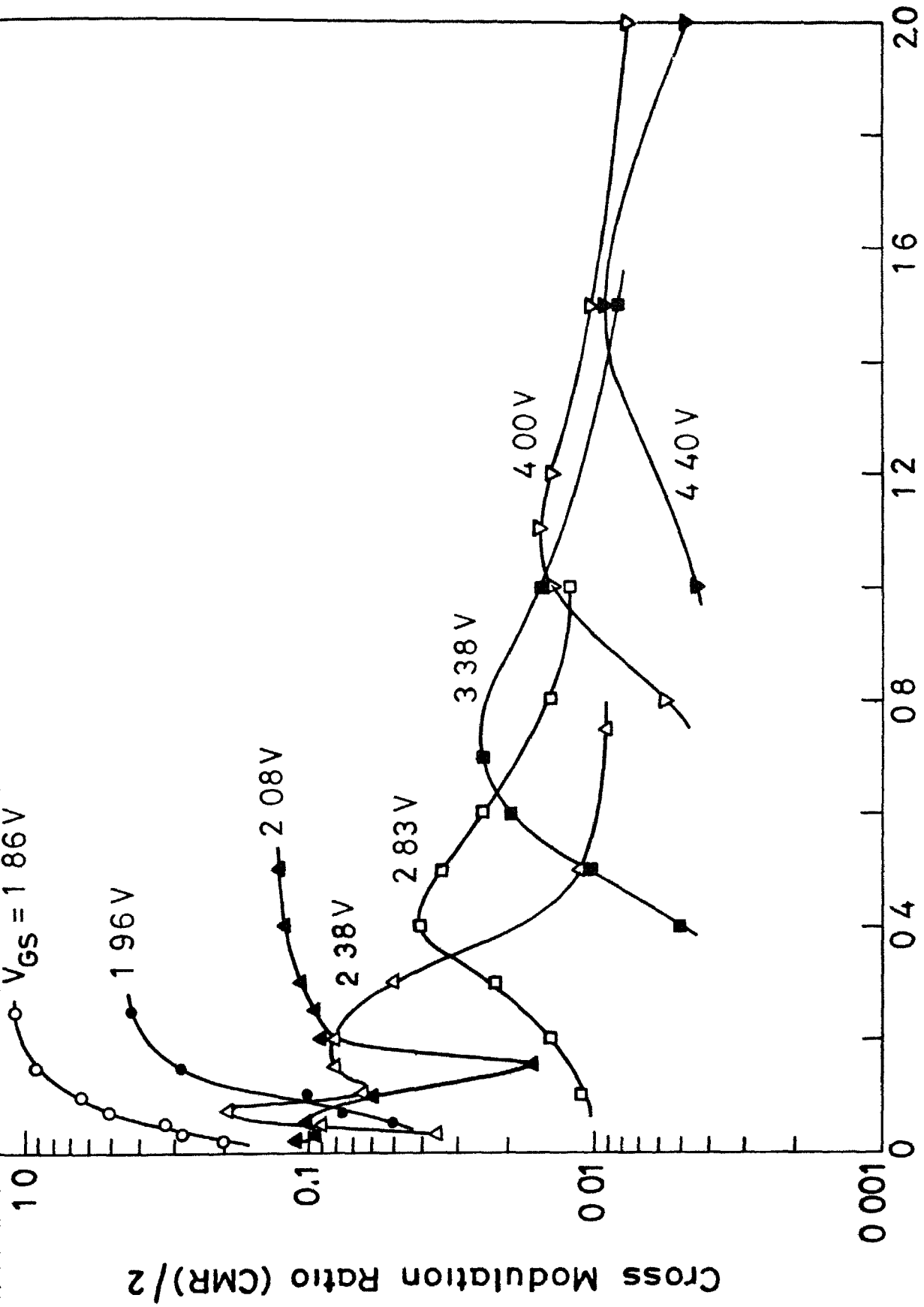

Fig 26 Cross modulation characteristic versus V_{DS}

MOSFET. The experimental part of the measurement of cross modulation has also been described.

CHAPTER III

EXPERIMENTAL RESULTS AND COMPUTER SIMULATION

The discussion in the previous chapter emphasized the importance of cross modulation for describing the nonlinearity of MOSFET. In the present chapter it will be shown that from the cross modulation experiment, we can extract some information about the device, which can be used for modelling purposes.

We shall also see how the presently available models describe the nonlinear behaviour of MOSFET. We simulated the cross modulation in MOSFET using SPICE. Simulation part is given in the second section of this chapter. And finally the simulated characteristics are compared with the experimental ones.

3.1 MODELLING OF MOSFET

Today's MOSFET models lack the level of precision required for aggressive analog circuit design. The problems encountered for this purpose are presented in the discussion that follows. Our experimental results are then discussed in this context.

3.1.1 Drain Current Expression

Single expressions valid in all regions of operation have been developed by considering both drift and diffusion

[9,10]. Such expression avoid artificial transition from one region to the next, and the corresponding large errors in calculating small signal parameters. The double integral form proposed by Pao-Sah [9] comes in excellent agreement with experiments [10] but the need of complex numerical calculations makes it impractical for actual circuit design [11]. The mathematical complexity of the very general formulation [9] can be reduced by assuming a 'charge sheet model' [10], however, the resulting expression give the drain current in terms of surface potentials rather than terminal voltage, in the form

$$I_{DS} = -\mu \left(\frac{W}{L}\right) \int_{\psi_{SO}}^{\psi_{SL}} Q'_I (\psi_s) \frac{dV}{d\psi_s} \, d\psi_s \qquad (3.1)$$

where ψ_s is the surface potential, ψ_{so} and ψ_{sL} its value at the source and drain end of the channel respectively, Q'_I is the inversion layer charge per unit area, and V is the electron quasi Fermi potential with respect to the bulk Fermi level. No accurate explicit general expression is available [12] for the ψ_s as a function of V, approximate such expressions are available for the special cases of weak and strong inversion, region, but not for the region in between.

3.1.2 Moderate Inversion

In view of the high complexity of the formulation discussed above, using different equations for different regions of operation still seems necessary for computational

efficiency. However, popular CAD models make an assumption which is too crude for analog work that common weak and strong inversion expressions are valid in adjacent regions [12]. To examine this assumption, let us consider a very small V_{DS}. A linear variation of I_D with V_{GS} would imply a constant transconductance g_m and the exponential variation (in weak inversion region) would instead imply a constant g_m/I_D. Thus g_m and g_m/I_D can be used as sensitive indicators of haw straight or exponential $I_D(V_{GS})$ really is. A typical plot of these indicators, normalized to their maximum value, is shown in Fig. 3.1 [13]. It shows that there clearly exists a region where $I_D(V_{GS})$ is neither exponential nor a first degree term. This region is called moderate inversion.region. Attempts to calculate g_m in this region by using either strong or weak inversion common expressions can result in very large error. The width of the moderate inversion region is hundreds of millivolts, its exact value being dependant on process parameters and source-to-substrate bias.

3.1.3 Precision Modelling

It is clear from the above discussion that for critical applications where an accurate small signal analysis is needed or where we want to predict nonlinear parameters of a circuit, the subtle nuances of the I-V characteristic must be maintained Currently, distortion is predicted inaccurately by some CAD programs [12].

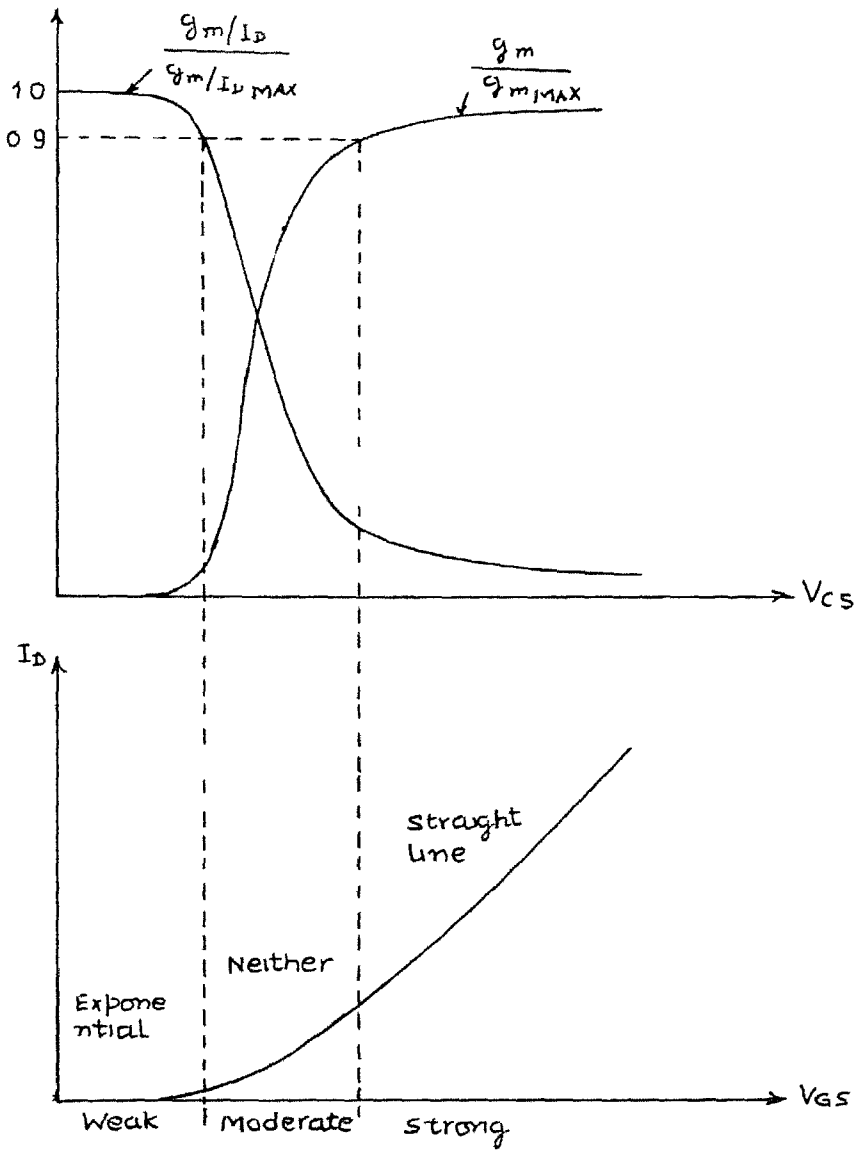

Fig 3 1 Device characteristics versus V_{GS}, for small V_{DS} (a) Transconductance and transconductance -to-current ratio, normalised to their maximum values (b) Drain current

The cross modulation experiment, described in the last chapter can be used to accurately describe the behaviour of MOSFET inmoderate inversion region. We can also see the variations of the I-V characteristic in different regions.

3.1.4 Nonlinearities in the MOSFET

Cross modulation is mainly caused due to the third order nonlinearity of device [14], as we have seen in the previous chapter. If we take another view of the same fact, we can explore those regions of operations of MOSFET where cross modulation is significant. The results can then be utilized for physical characterization of the nonlinearity of device.

The curves given in Fig. 2.5 and 2.6 indicate large value of cross modulation ratio in the moderate inversion region and surprisingly in the linear region also. As V_{GS} is increased in the moderate inversion region, CMR decreases due to transition from exponential to square law characteristic. We get two peaks in this characteristic, one in the weak inversion region and other in the linear region. (The peak in weak inversion region is not visible in Fig. 2.5 because accurate measurements could not be made below some particular value of V_{GS} due to some experimental difficulties).

The first order component and the third order components of the $I_D - V_{GS}$ characteristics have been plotted in Fig. 3.2(a) to

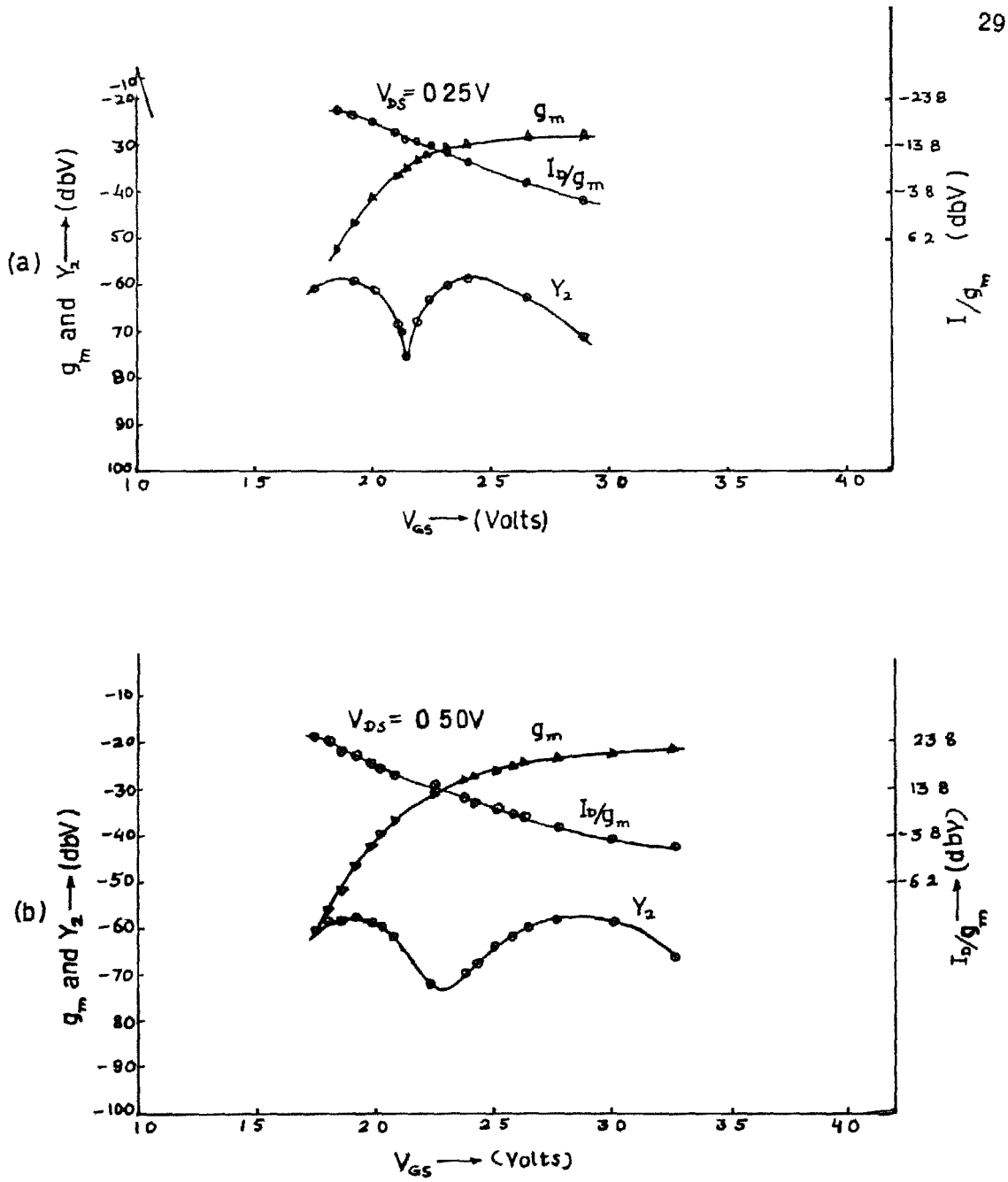

Fig 3 2 I_D/g_m and I st and III rd order components for
(a) V_{DS}= 0 25 V (b) V_{DS}= 0 50V [contd]

(c)

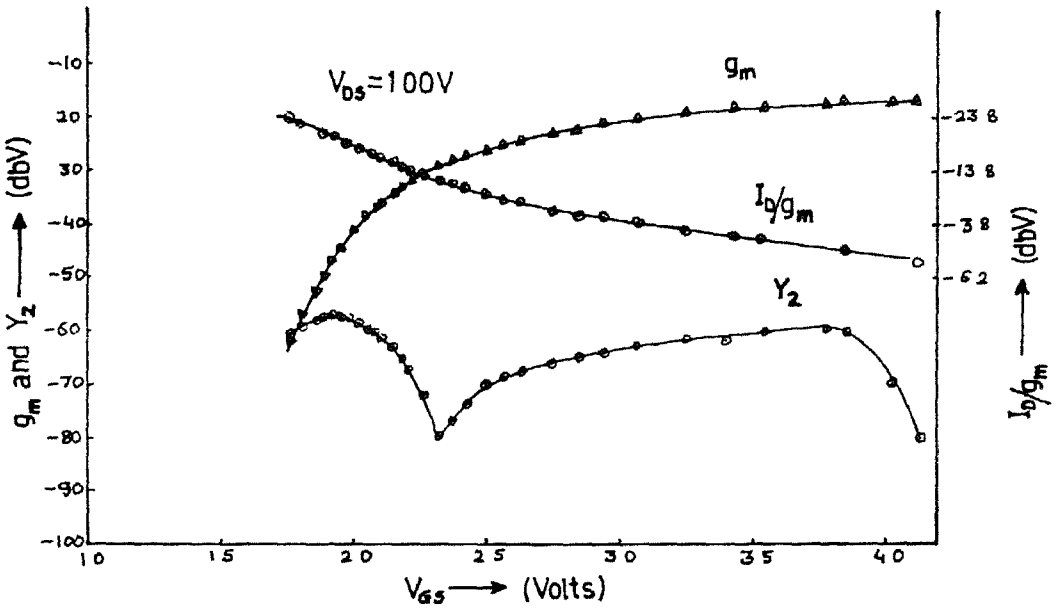

(d)

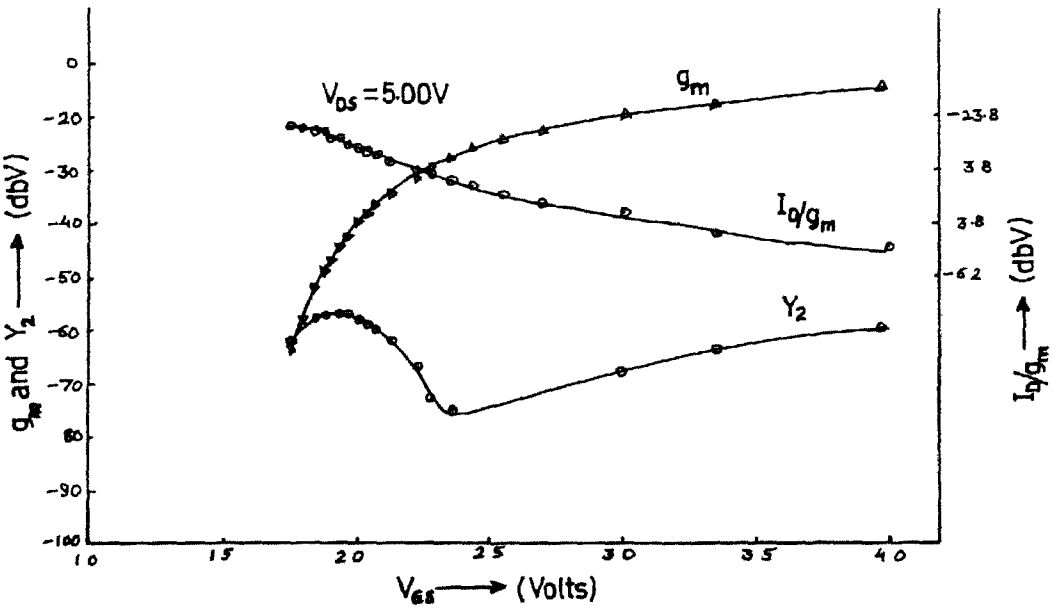

Fig 3 2 I_D/g_m and, Ist and IIIrd order components for

(c) V_{DS}=100V (d) V_{DS}=5 00V

Fig. 3.2(d) These four figures are corresponding to different values of V_{DS} which are 0.25, 0.50, 1.0 and 5.0. We have also plotted the ratio of current to transconductance in these figures. The features revealed from these curves are as follows :-

1) $g_m - V_{GS}$ characteristic does not become constant in the linear region abruptly. The current transconductance ratio also becomes constant well within the weak inversion region. This shows that there does exist a region like moderate inversion region where the behaviour of the device can not be described by either of the characteristics of the adjacant regions.
2) The third order component assumes one peak in the moderate inversion region and the other in the linear region, the value being almost same in both the regions. The nonlinearity of MOSFET in the linear region can be seen more clearly from Fig. 2.6. This shows that the behaviour of the device can not be described by simple equation in the linear region. For accurate modelling the higher order terms can not be neglected.
3) The variation of the first order and third order components can be used to model the device in the moderate inversion region. Suitable approximation can be made in the general Pao-Sah model [9] to arrive at an analytic equation in this region. The parameters needed for this can be extracted from cross modulation measurement.

4) The cross modulation measurements can be used for parameter extraction of MOSFET. The points of inflection of the derivatives of the I-V characteristic can be found very accurately using these measurements. If we can theoretically find them from the general Pao-Sah equation, some parameters of the device can be extracted, which can be used to accurately describe the behaviour of the device in all the regions.

3.1.5 Approximations made in the Experimentation

We have made certain approximations in the experimental work done so far. Let us have a look at them and their validation before concluding this section.

We have neglected the contribution resulting from the fifth order and higher order nonlinearities of the device. This assumption is valid only if (1) the device is weakly nonlinear and (2) input signal amplitude are small enough. This was verified using the intermodulation behaviour of the device.

If we give a two tone input (frequencies f_1 and f_2) to the MOSFET, then at the output we shall get intermodulation components at f_1, f_1+f_2 and $2f_1-f_2$ due to the frequency mixes (0010), (0011) and (1020) respectively. If the higher order nonlinearities are negligible then for the case of equal available powers of the input tones, these intermodulation components should be proportional to the input powers, with the constant of proportional equal to the order of the nonlinearity

due to which they are being produced. These three intermodulation components are plotted in Fig. 3.2 with respect to the input signal level. Fig. 3.3(a) corresponds to the operation of the MOSFET in weak inversion region and Fig. 3.3(b) to the linear region.

The input signal levels used at $f_I - f_m$, f_I, $f_I + f_m$ and f_s are -12 dbV, -22 dbV, -12 dbV and -28 dbV respectively (0 dbV = 1 V). These values were choosen in such a way that nonlinearities due to rest of the circuit andspectrum analyzer are negligible. They were kept constant thoughout the experimentation. Fig. 3.2 shows that these levels of input signals lie almost in the linear range of the intermodulation characteristics.

3.2 SIMULATION OF CROSS MODULATION

Many authors have computed cross modulation in FETs using the power series expansion of the device transfer characteristic [2 3,5]. But o approach was to extract some information about the device behaviour, and to correlate the nonl rear behaviour to the basic device equations describing the device model. So we calculated cross modulation in MOSFET using SPICE.

For SPICE simulation, we first found the parameters of the device used in cross modulation. The procedures followed for the purpose are described in the following subsection.

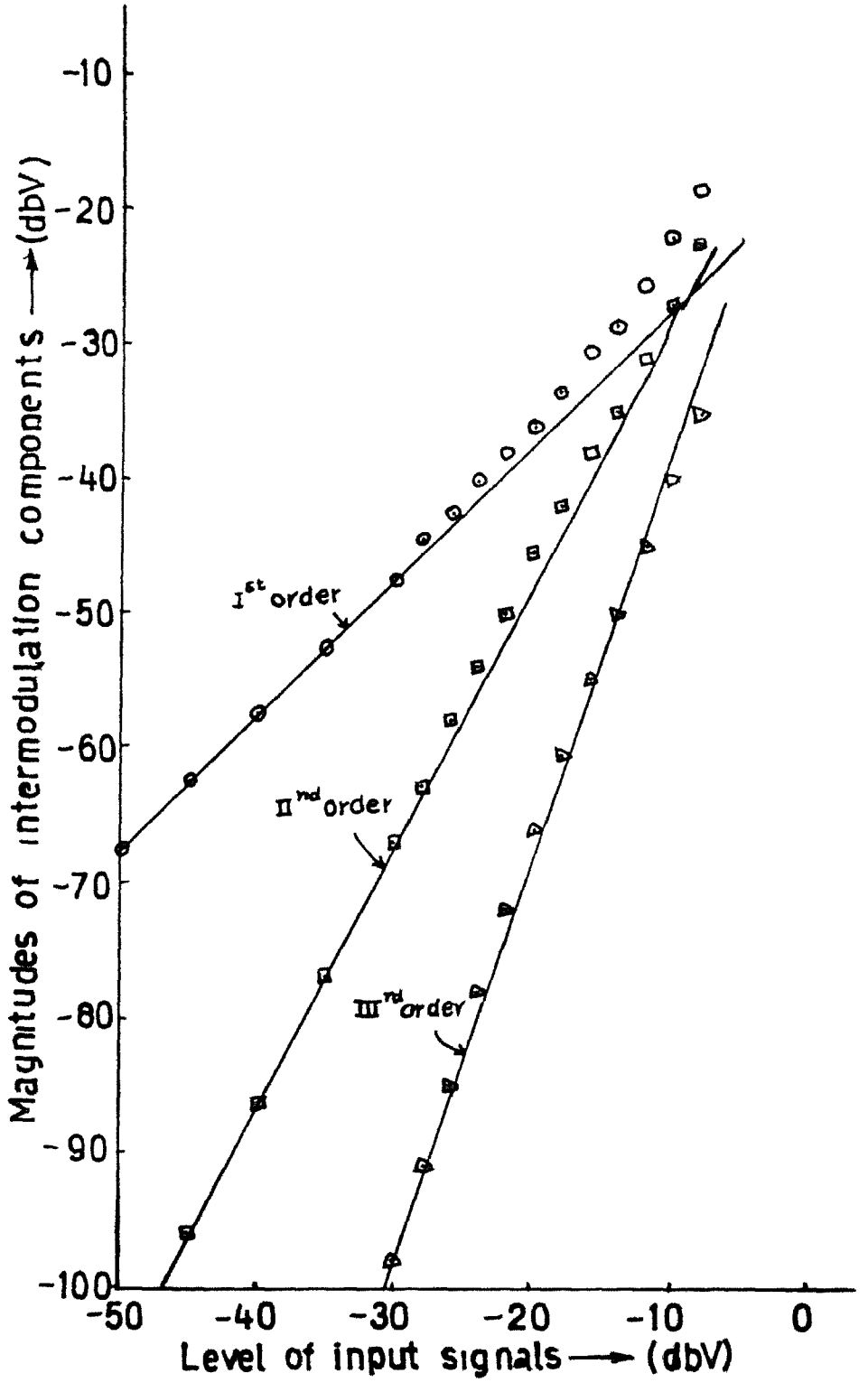

Fig 3 3 Intermodulation behaviour for checking the input signal levels
(a) in weak inversion

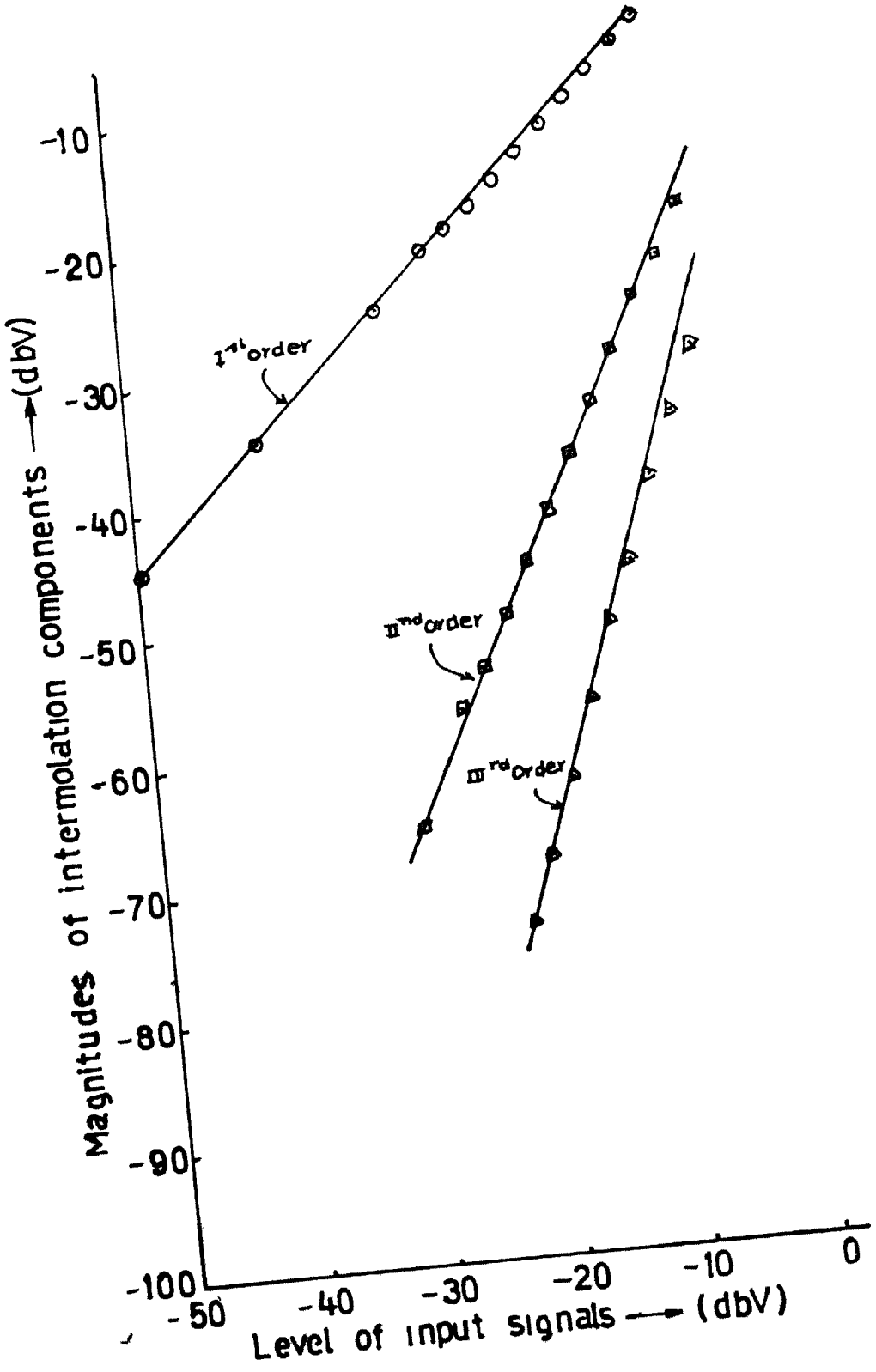

Fig. 33(b) in strong inversion

Besides SPICE, some more software are necessary for cross modulation simulation. This is discussed in next part of this section before the description of the results of cross modulation simulation

3.2.1 Parameter Extraction for SPICE

We specified only the necessary parameters for SPICE to avoid unnecessary complications. LEVEL = 1 model of SPICE was not sufficient for our purpose since it does not take into account the weak inversion conduction of the device. So we used LEVEL = 2 model. The parameters specified for this are given below, with the method used for their measurement:

(i) VTO (zero-bias threshold voltage) and KP (transconductance Parameter)

The square law behaviour of MOSFET was used for the evaluation of these two parameters. I_D V/S $V_{GS}(= V_{DS})$ characteristics of MOSFET was measured in saturation region and $\sqrt{I_D}$ was plotted as a function of V_{GS}, as shown in Fig. 3.4. The slope of the straight line joining these data points gives the value of KP and the intercept of the line with the horizontal axis gives VTO. Thus we obtained KP = 3.8×10^{-3} A/V^2 and VTO = 1.875 V.

(ii) NFS (Surface State Density) and NSUB (Substrate Doping)

These two parameters were measured using the current measurement in the weak inversion region. The current

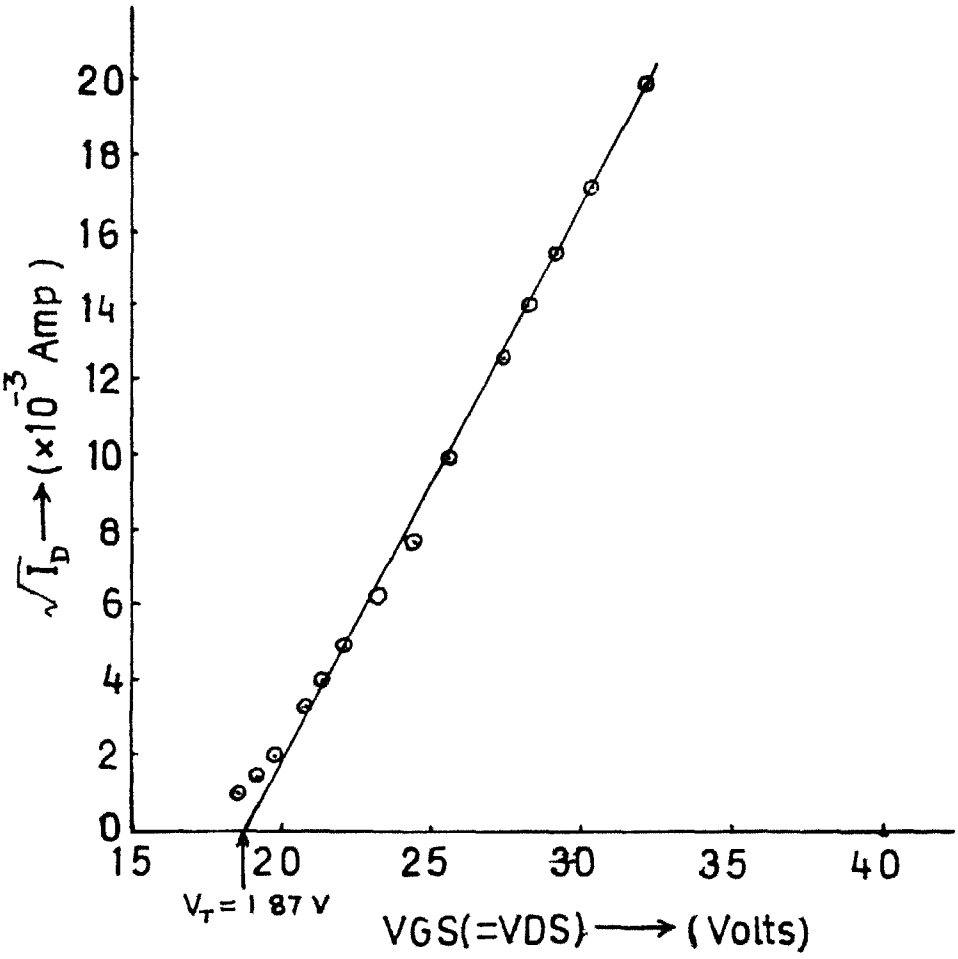

Fig 3.4 Threshold and transconductance parameters measurements

behaviour in this region has been a subject of extensive analysis by Pao and Sah [9] and Swanson and Meindl [15]. It has been established that for gate voltage V_G and drain voltage V_D, the drain current in this region is given by [15]

$$I_{DS} = \frac{W}{L} \mu \frac{C_{ox}}{m} \left(\frac{n\,kT}{q}\right)^2 \exp\left[\frac{(V_{GS} - V_T)}{nkT} q\right]\left(1 - e^{-\frac{m\,q\,V_{DS}}{nkT}}\right) \quad \ldots\ldots \quad (3.2)$$

So, for fixed V_{DS},

$$I_{DS} = I_O \exp\left[\frac{(V_{GS} - V_T)}{nkT} q\right] \quad (3.3)$$

and for fixed V_{GS},

$$I_{DS} = I'_O \left(1 - e^{-\frac{m\,q\,V_{DS}}{nkT}}\right) \quad (3.4)$$

where L = Channel length

W = Channel width

C_{ox} = Oxide capacitance

μ = Surface mobility

$$m = \frac{C_{ox} + C_D}{C_{ox}} \quad (3.5)$$

$$n = \frac{C_{ox} + C_D + C_{FS}}{C_{ox}} \quad (3.6)$$

and C_D and C_{FS} are capacitances associated with the depletion layer and fast surface states respectively. If C_D and C_{FS} can be found, the required parameters can be found by

$$C_D = \frac{q \in_s . NSUB}{4\,|\phi_p|} \quad (3.7)$$

and $C_{FS} = q.NFS$ (3.8)

Equation (3.3) shows that n can be found by I_{DS} V/S V_{GS} plot. We measured I_{DS} as a function of V_{GS} using the same set-up as described in the last chapter. The values are plotted in Fig. 3.5 on semilog scale. A straight line was fitted in the below threshold region. The slope of this line gave value of n = 2.67.

Similarily we measured I_{DS} as a function of V_{DS} for fixed V_{GS} and plotted $(1 - \frac{I}{I'_0})$ with respect to V_{DS}, as given in Fig. 3.6. (I'_0 is equal to the value of I_{DS} for large value of V_{DS}). The slope of the curve fitted straight line gave the value of m = 2.16.

Using eq. (3.5) and (3.6) we found $C_D = 3.48 \times 10^{-8}$ F/cm^2 and $C_{FS} = 1.53 \times 10^{-8}$ F/cm^2. Then eq. (3.7) and (3.8) were used to calculate the values of NSUB and NFS respectively. The values thus obtained are NSUB = 1.11×10^{16} cm^{-3} and NFS = 9.56×10^{10} cm^{-2}.

(iii) <u>W (Channel Width) and L (Channel Length)</u>

The values of these parameters were measured in our lab. using SEM after opening the chip. We used the same values for simulation purpose. These are : W = 175 μ and L = 12.5 μ, Tox = 100Å

Since the device dimensions are quite large, there was no need of specifying those parameters which describe small geometry behaviour of MOSFET.

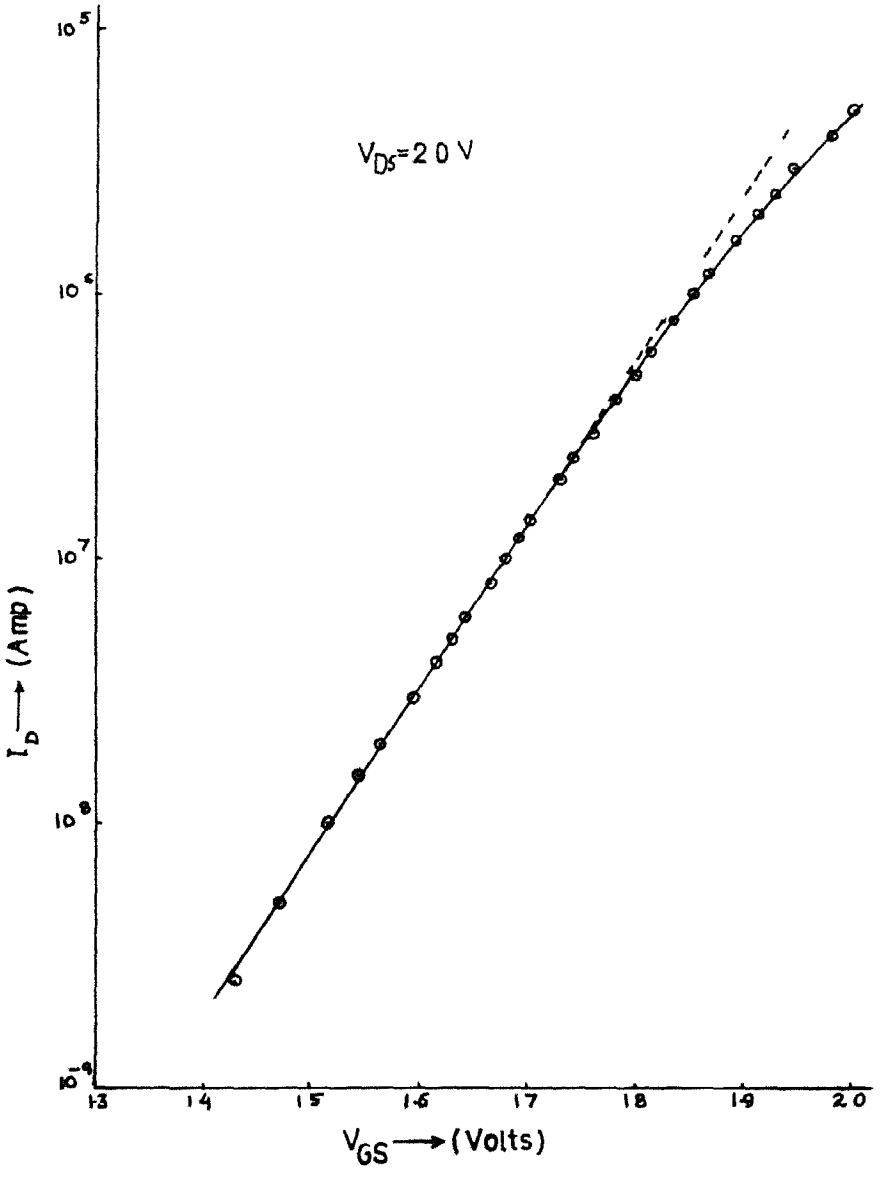

Fig 3.5 Subthreshold current measurement for finding 'n'

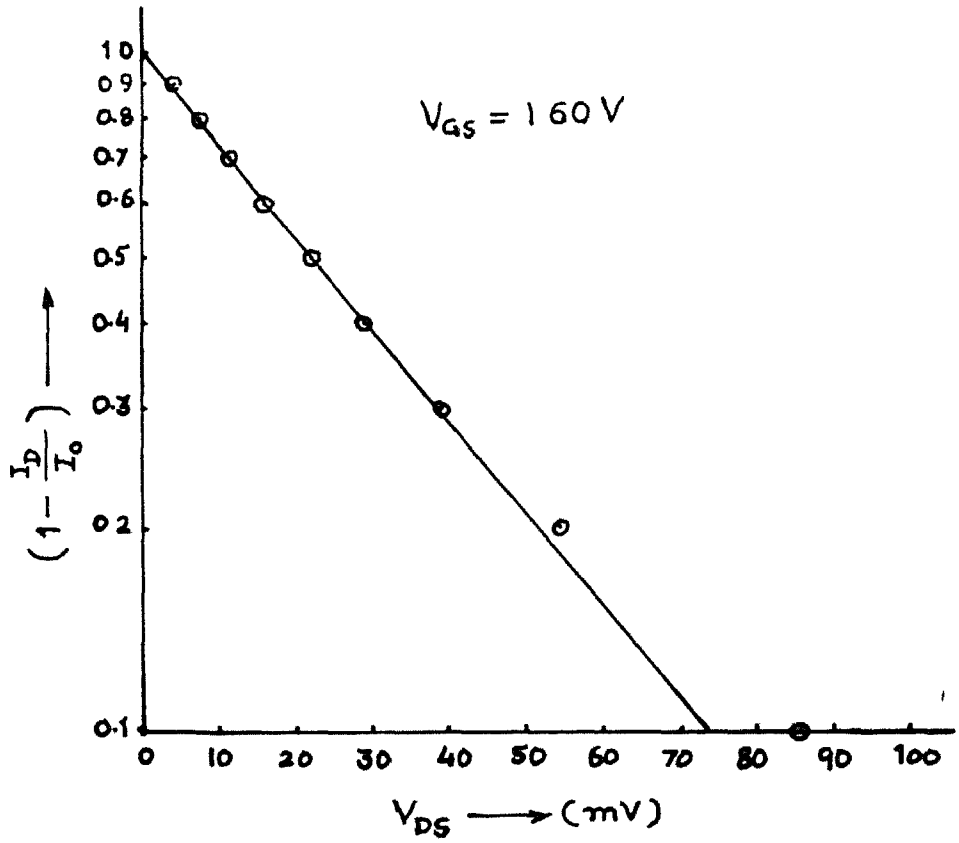

Fig 3.6 Subthreshold current measurement for finding 'm'

3.2.2 Software Development

We made two programs which, in combination with SPICE, were used for simulating the cross modulation behaviour of MOSFET. A block diagram of the three programs with their main function is given in Fig. 3.7. It shows how they are used one after another, to find out CMR. The programs IMOD and PDFT are described below with the steps of their developments

(i) IMOD

This program was used as a tool for selection of the frequencies of the input signals (modulated and unmodulated) for cross modulation simulation. In lab. experimentation on cross modulation, this selection was not a big problem since we could vary the input frequencies smoothly (in analog fashion). There are some constraints in the software simulation which will be discussed later.

It was shown in the last chapter that for a Q frequency input, the output due to the n^{th} order transfer function of a nonlinear circuit extends over (eq. (1.12) repeated here)

$$M = \frac{(2Q - n - 1)!}{n!\,(2Q - 1)!} \qquad (3.9)$$

distinct mix vectors. For example, in response to four input frequencies, the third order portion of the system will generate sinusoidal components corresponding to 60 distinct frequency mixes

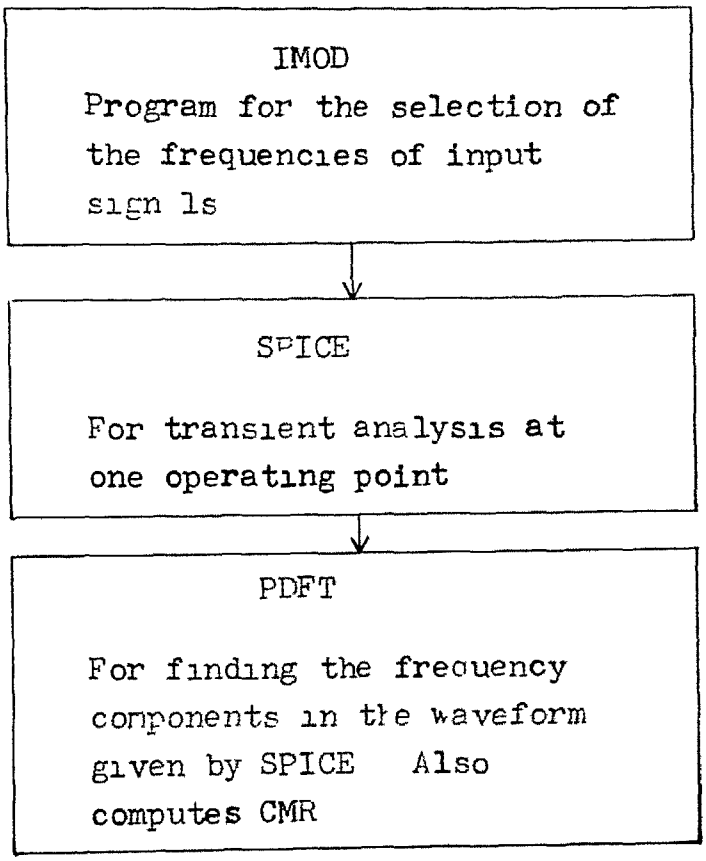

Fig 3.7 Block diagram of the software used for cross modulation simulation

We want that no other frequency mix should affect the output at the cross modulation frequencies ($f_s - f_m$ and $f_s + f_m$), except the two listed in Table 2.1 (No. 6 and 7).

The inputs to be given to the program IMOD are as follows .-

1) Input frequencies (maximum five frequencies can be specified).
2) Maximum order of nonlinearity to be taken into account (maximum value 7).
3) The output frequencies to be observed (maximum value 12).

In the output, the program gives the mix vector of the input frequencies affecting at the output frequencies to be observed (i.e. input No. 3). It also gives the order of nonlinearity corresponding to those mixes.

(ii) PDFT

This program calculates the Discrete Fourier Transform (DFT) of the sample points of the waveform given by SPICE output. Thus we estimate the Fourier Series coefficient of the output waveform by DFT.

The DFT coefficients estimate the Fourier Series coefficients very well only if some conditions are satisfied [16], some of which are as follows -

1) The waveform should be band-limited which implies nonzero Fourier Series coefficients for $-N/2 < m < N/2$ where N is the number of sample points of the waveform. If this condition is not met, the out of band components distort the computed spectrum.

2) There should not be any component in the 'actual' spectrum of the waveform which comes in between the frequencies of the components given by the DFT. This requires that the waveform should repeat after the time upto which sample values are given to the program.

Care was taken to fulfil these condition as described in the next subsection.

The program PDFT takes its input from the output file produced by SPICE. It uses FET algorithm (CØ6FAF) of NAG subroutine library. In the output, PDFT gives the magnitude of the DFT components and the frequencies corresponding to them. It also gives the normalized magnitude of all the components with respect to the magnitude of a frequency component specified interactively. We specified the component corresponding to the frequency f_s (please refer to Fig. 2.3) for notation) for normalization. Thus we get the normalized magnitude of spectral components at $(f_s \pm f_m)$ equal to cross modulation ratio (CMR)/4.

3.2.3 Simulation Results

The selection of input frequencies for cross modulation was done using the program 'IMOD'. The input frequencies had to be choosen under the following constraints .-

1) They should be multiple of the frequency corresponding to the time upto which sample value of waveform are taken. In SPICE we did transient analysis upto 1 msec only, so all frequencies should be multiple of 1 KHz.

2) The maximum input frequency should be lessthan about one/ fourth of the maximum frequency component calculated by DFT. This is necessary to approximately fulfill the condition of bandwidth limitation for DFT estimation of Fourier Series coefficients.

We tried several combinations under the above mentioned constraints, to arrive at the final selection which is f_1 = 25 KHz, f_2 = 15 KHz, f_3 = 14 KHz and f_4 = 16 KHz. The frequency mixes affecting at 8 output frequencies of interest are given in Table 3.1. The extraneous components upto fourth order have been eliminated in the output at frequency $f_s - f_m$. Since our input frequencies are low enough, the cross modulation components Y_2 and Y_3 are expected to be same. We used the output at the frequency $(f_s - f_m)$ only to find out CMR.

In the SPICE input, we gave four sinusoidal signals of the four frequencies found using IMOD, three corresponding to the modulated signal and the fourth one to the unmodulated signal. The program SPICE and PDFT were run one after the other to find out cross modulation at one operating point. This was repeated for different operating points at a particular drain voltage V_{DS} (varying V_{GS}). The results thus obtained for V_{GS} = 0.25 V are given in Fig. 3.8(a).

These calculations were done on the parameters of the device calculated by us. To see the effect of the variation of parameters on cross modulation, we changed NFS to 1.00×10^{10} cm^{-2}

TABLE 3 1 M[illegible] (f[illegible] ML)

HL FREQUENCIES OF INPUT TONES

0 2500E+05 Hz   0 1500E+05 H   0 1 00E+05 HL   0 1 00E+05 Hz

REQUIRED INTERMODULATION COMPONENT	ORDER	M VECTOR							
FREQUENCY= 0 1400E+05 Hz									
	1	0	0	0	0	0	0		0
	3	1	0	0	0	0	2	0	0
	3	1	0	0	0	0	0		1
	3	0	1	0	0	0	0	2	0
	3	0	0		0	0	1		0
	3	0	0	0	1	1	0		0
	[illegible]	2	0	0	0	0	2	0	
	5	[illegible]	0	0	0	0	0	1	[illegible]
	5			0	0	0	2		0
	5				0	0	0	2	
	5	1	0	1	0	0	3	0	0
	5	1	0		0	0	1	1	1
	5			0	1		2	0	0
	5		0	0		1	0		
	5	0	2	0	0	0	0	[illegible]	0
	5	0		1	0	0	1	2	0
	5	0			1		0	2	0
	5	0	0	2	0	0	2		0
	5	0	0	2	0	0	0	2	1
	5	0	0	1		1	1	1	0
	5	0	0	0	2	2	0	1	0
FREQUENCY= 0 1500E+05 Hz									
	1	0	0	0	0	0		0	0
	3		0	0	0	0		0	1
	3	0	1	0	0	0			
	3		0	1	0	0	2	0	0
	3	0	0		0	0	0	1	
	3	0	0	0			1	0	0
	5	2	0	0	0	0	1	0	2
	5	1		0	0	0	3	0	0
	5	1	1	0	0	0	1	1	1
	5		0		0	0	2	0	1
	5	1	0		0	0	0		[illegible]
	5	1	0	0			1	0	
	5	0	2	0	0	0	1	2	0
	5	0		1	0	0	2		0
	5	0	1	1	0	0	0	2	
	5	0	1	0	1	1	1	1	0
	5	0	0	2	0	0	3	0	0
	5	0	0	2	0	0	1	1	1
	5	0	0	1	1	1	2	0	0
	5	0	0	1	1	1	0	1	1
	5	0	0	0	2	2	1	0	0
FREQUENCY= 0 1600E+05 Hz									
	1	0	0	0	0	0	0	0	1
	3		0	0	0	0	0	0	2
	3	0	1	0	0	0	2	0	0
	3	0	1	0	0	0	0	1	1
	3	0	0	1	0	0	1	0	1
	3	0	0	0	1	1	0	0	1
	5	2	0	0	0	0	0	0	3
	5	1	1	0	0	0	2	0	
	5	1	1	0	0	0	0	1	2
	5		0	1	0	0	1	0	2
	5	1	0	0	1	1	0	0	2
	5	0	2	0	0	0	[illegible]	1	0
	5	0	2	0	0	0	0	2	
	5	0	1	1	0	0	3	0	0
	5	0	1	1	0	0	1	1	1
	5	0	1	0	1	1	2	0	0
	5	0	1	0	1	1	0	1	1
	5	0	0	2	0	0	2	0	1
	5	0	0	2	0	0	0	1	2
	5	0	0	1	1	1	1	0	1
	5	0	0	0	2	2	0	0	1

TABLE 3 1(Cortd)

FREQUENCY= 0 2500E+05 Hz

3		0	0	0	1	^	1	0
4	0	^	^		^	0	0	3
5	2	0	^	0	1	2	^	^
5	2	0	^	^	1	0	1	1
5		1	0	0		0	2	^
5	1	^	1	0		1	1	0
5	^	0	^	1	2	0	1	0
5	^	^	2	0	1	^	2	0

FREQUENCY= 0 2600E+05 Hz

3	^	^	^	^	1	1	^	^
3	^	^	^	^	1	^	1	^
5	2	^	0	^	1		^	
5		1	0	^	1	1		^
5		^	1	^	1	2	^	^
5		^	1	0	1	^		
5		^	^	1	2			
5	0	1	1	0	1	0	2	^
5	0	^	2	^	1	1	1	^
5	^	^	1	1	2	^	1	0

FREQUENCY= 0 2500E+05 Hz

	^	0	^	0	1	0	0	0
3	1	0	^	^		^	0	
3	^	1	^	^	1	^		^
3		^		^			^	^
3	^	^	^		2	^	0	^
5	2	^	0	0	1	0	0	2
5	1		^	0		2	0	^
5			^	^	1	0	1	
5	1	^	1	0			^	1
5	1	^	0	1	2	^	^	
5	^	2	0	^	1	^	2	^
5		1		^				^
5	^	1	^		2	^		^
5	^	^	2	^	1	2	0	^
5	0	^	2	0	1	0	1	1
5	0	0	1	1	2	1	0	^
5	^	0	0	2	3	0	^	^

FREQUENCY= 0 2600E+05 Hz

3	0	1	0	0	1		0	0
3	0	0	1	0		^	0	1
4	1	0	0	^	^	^	3	^
5	1	1	0	0	1	1	0	1
5	1	^	1	0	1	0	0	2
5	0	2	0	0	1	1	1	0
5	0	1	1	0	1	2	^	^
5	0	1	1	^	1			1
5	0	1	0	1	2	1	0	^
5	0	0	2	0	1	1	0	1
5	0	0	1	1	2	0	0	1

FREQUENCY= 0 2700E+05 Hz

3	^	1	0	0	1	^	0	
4	1	0	^	0	0	1	2	0
4	0	0	1	0	0	^	3	0
5	1	1	0	0	1	^	0	2
5	0	2	0	0	1	2	0	0
5	0	2	0	0	1	0	1	
5	0	1	1	0	1	1	^	1
5	0	1	0	1	2	^	^	1
5	0	0	2	0	1	0	0	2

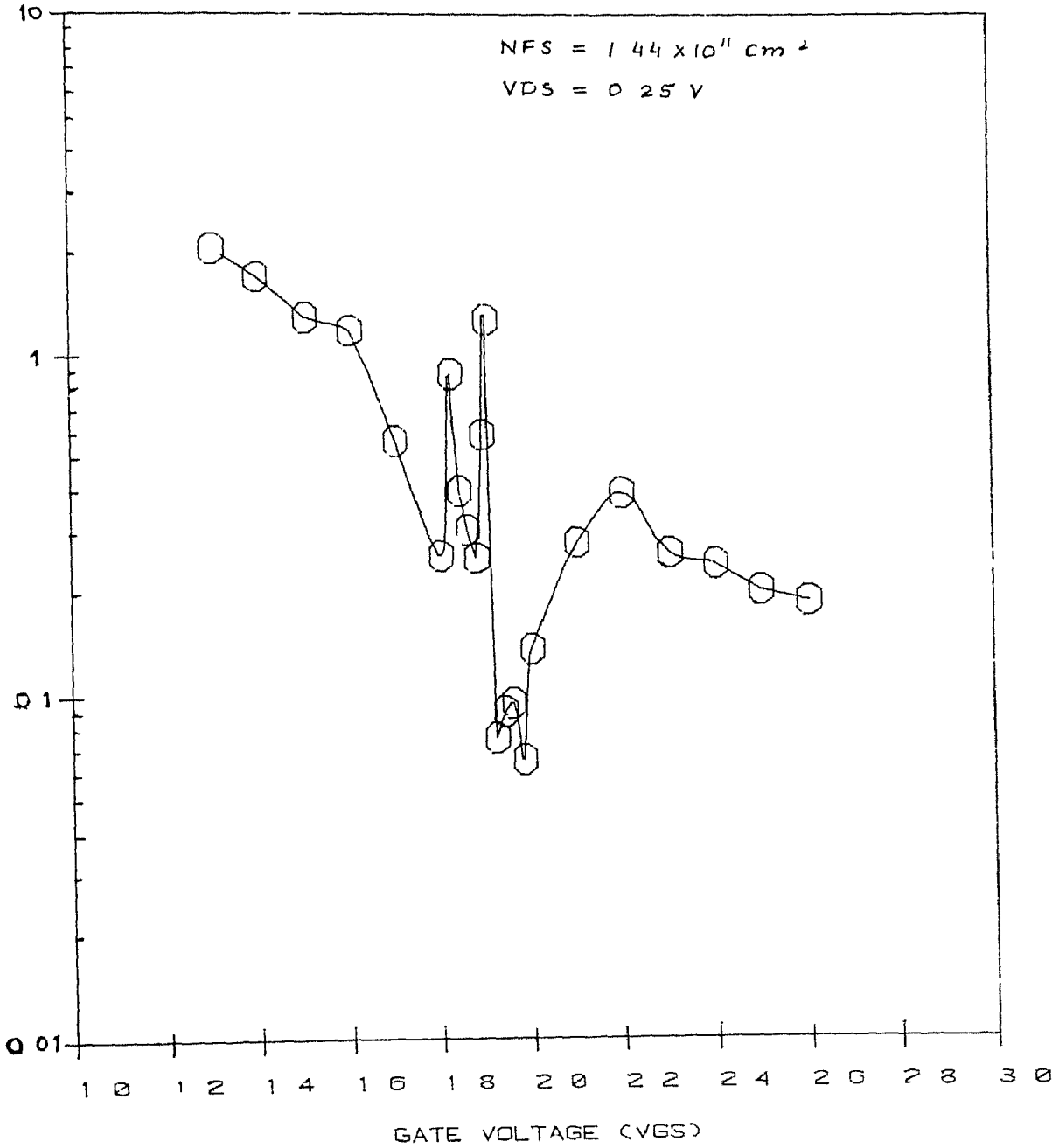

Fig 38(a)
SIMULATED CROSS-MODULATION CURVE

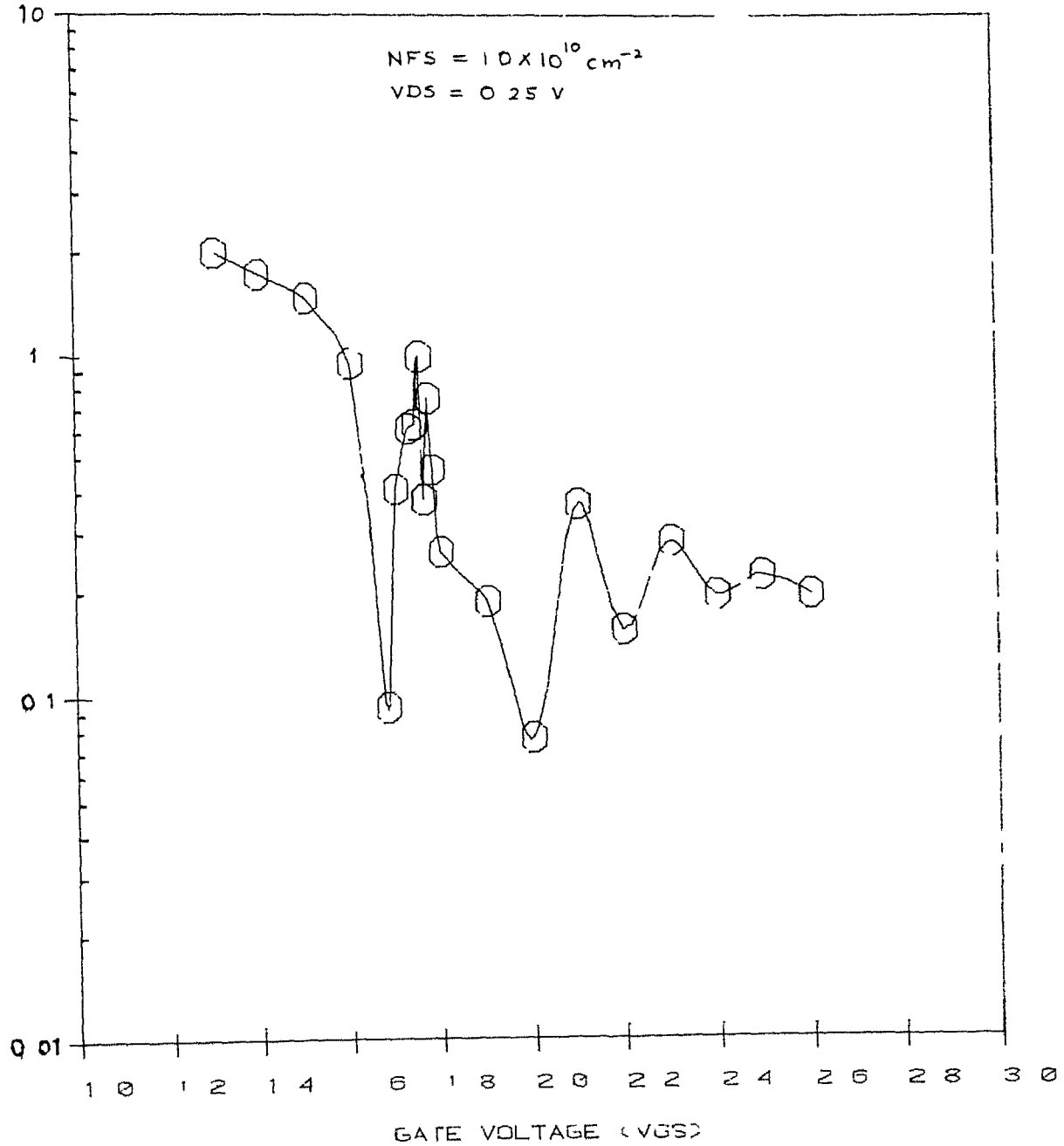

Fig 3 8(b)

SIMULATED CROSS-MODULATION CURVE

and plotted the CMR V/S V_{GS} curves for same value of V_{DS}. This is shown in Fig. 3.8(b).

The results thus obtained are compared in the next section with the experimental ones.

3.3 COMPARISON BETWEEN THE EXPERIMENTAL AND SIMULATION RESULTS

The cross modulation curves obtained by SPICE simulation (Fig. 3.8) show qualitatively almost the same features as those obtained by experiments (Fig. 2.5). We get high value of cross modulation in weak inversion region in both the curves and then we get another peak also at higher value of gate voltage. But if we observe them closely we can note the following differences :-

1) The simulated curves do not have the same smooth variations as those obtained by experiments.
2) We get large fluctuation in the CMR value near the peak of the curve.
3) The values of CMR are almost the same in the weak inversion region for the simulated and experimental curves, but they differ substantially, in other regions.

The differences between the experimental and simulated curves can be attributed to the device equations used in the SPICE model. It may be that the device model cannot correctly account for the nonlinear effects.

For simulation of the nonlinear behaviour of MOSFET, the right approach seem to be the one adopted by Meyer [1].

in which they curve-fit the measured $g_D - V_{GS}$ characteristic to get $I_D - V_{GS}$ characteristic and thus retain the higher order terms. But this approach will not do for CAD purposes, where a general purpose model is required to work for all the regions of operations. This demands precision modelling of the MOSFET. We have suggested a method to describe the behaviour of the MOSFET in moderate inversion, where recent models have failed. We have also seen how current models like SPICE do not describe the nonlinear behaviour of the device. Further work needs to be done for precision modelling of the MOSFET to accurately describe the nonlinear behaviour.

CHAPTER IV

FLICKER NOISE IN MOSFET

In this chapter the flicker noise in MOSFET's has been characterized. It is presently believed that the presente of electron energy states at $Si-SiO_2$ interface gives rise to an input referred flicker noise component that is larger then the thermal noise component for frequencies below 1 to 10 KHz for most of the bias conditions and device geometries. In this chapter attempt has been made to correlate the cross modulation behaviour with that of the flicker noise.

4.1 FLICKER NOISE IN WEAK INVERSION AND STRONG INVERSION REGIONS

Several models have been proposed to account for flicker noise in MOSFET, the most common being the mobility fluctuation model (usually described by Hoge's empirical relation) and McWhorter's model (which assumes tunneling transitions between traps in the oxide and channel charges). Reimbold [17] has used McWhorter's model to explain the behaviour of noise in weak inversion and strong inversion regions. The general relation valid for input referred power spectral density in weak and strong inversion regionsis

$$S_{ID}(f) = \frac{K}{f^{\gamma}} \frac{N_t}{(C_{ox} + C_D + C_{FS} - \beta Q_n)^2} \cdot I_D^2 \qquad (4.1)$$

where $K = \frac{q^2 \lambda}{WL\, kT}$

$\beta = kT/q$

γ = frequency dependance constant of noise ($0.8 < \gamma < 1.2$)

N_t = trap density

C_{ox} = oxide capacitance

C_D = depletion capacitance

C_{FS} = interface trap capacitance

Q_n = channel charge

I_D = drain current

λ = tunneling constant for electrons

W and L are channel width and length respectively.

For strong inversion region $\beta Q_n >> C_{ox} + C_D + C_{FS}$ and

$$S_{ID} = \frac{K}{f^{\gamma}} \frac{N_t}{\beta^2 Q_n^2} I_D^2 \qquad (4.2)$$

For weak inversion region $\beta Q_n << C_{ox} + C_D + C_{FS}$ and

$$S_{ID} = \frac{K}{f^{\gamma}} \frac{N_t}{(C_{ox} + C_D + C_{FS})} I_D^2 \qquad (4.3)$$

From the above relations we can see that in strong inversion region S_{ID} is independant of I_D (since $Q_n \alpha I_D$) and in weak inversion region it varies as square of the magnitude of current. We probed into these two regions and the region in between (moderate inversion) through our measurements on noise.

4.2 MEASUREMENT OF NOISE

There is a wide variety of methods available for accurate measurement of noise · digital as well as analog. But we used simple oscilloscope method for this purpose. We did not use direct reading from scope because it results in erroneous reading for two reasons ·

1) Noise is highly random nature and is not sinusoidal Since rms values are required for noise calculations, the conversion from scope peak-to-peak values by $2\sqrt{2}$ is not accurate.
2) Since the noise peaks are random, their visibility on scope is influenced by such things as the scope's intensity setting, the persistence of CRT is phospher etc.

Because of the above reasons, we used another method known as tangential method for the measurement of noise. It has been claimed to be having error of less than 1 db [18]. In this method, noise signal is connected to both channels of a dual trace scope with alternate sweep capability. The vertical positions of the two beams are adjusted until the dark band between them just disappears. Then the noise signal input to both channels is removed. The resulting separation represents twice the RMS noise.

4.3 DESCRIPTION OF SET-UP

A block diagram of the set-up is shown in Fig. 4.1. Due care was taken to minimize the noise contributions due to

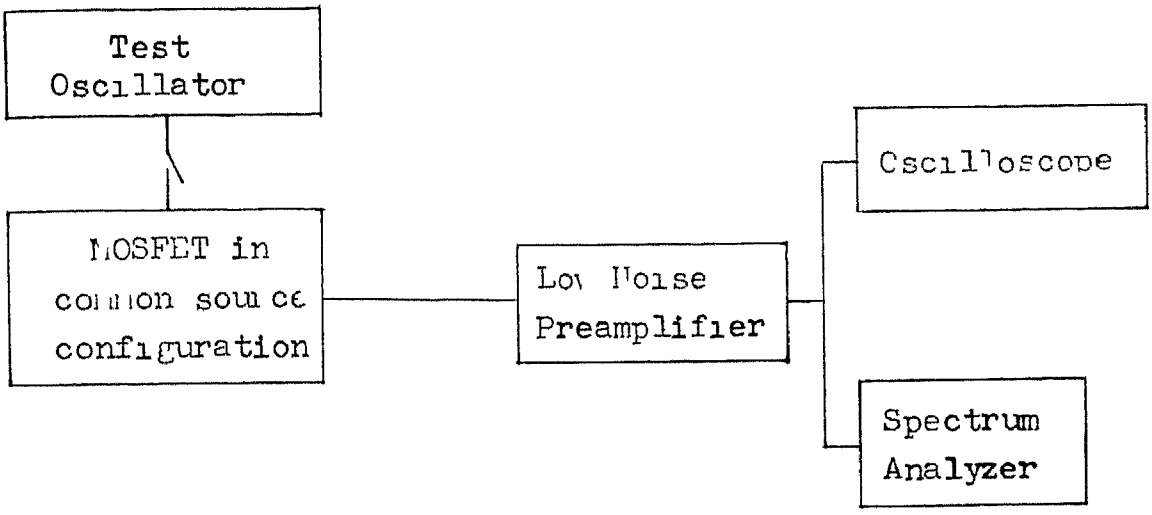

Fig 4 1 Experimental arrangement for measuring noise

amplifier, biasing circuit, power supply etc. To avoid interference effects, the biasing circuit was shielding using an iron box.

The noise of MOSFET was measured in common source configuration. To minimize the noise contribution due to the biasing circuit itself, we used simple resistor arrangement to bias the MOSFET.

The use of regulated power supply was giving rise to 50 Hz ripples with external noise components added to it. The order of magnitude of the noise to measured was of the order of few μV. No power supply available, could provide ripples of less than this order. So we resorted to the use of dry cells for biasing purpose.

As shown in the block diagram, we used a low noise preamplifier (NF model LI-75A) for amplifying the noise of MOSFET. It was AC coupled to the drain point of the MOSFET (cut-off frequency = 0.2 Hz), the input referred noise of this amplifier is 5 $nV/\sqrt{Hz}$ at 1 KHz.

4.4 EXPERIMENTAL RESULTS AND DISCUSSION

We measured the input referred noise of MOSFET at different bias points using the system described in Sec. 4.3. A typical spectrum seen on spectrum analyzer at a operating point is given in Fig. 4.2. At each operating point, test oscillator was connected to MOSFET for measurement of the system gain and disconnected while measuring noise. The

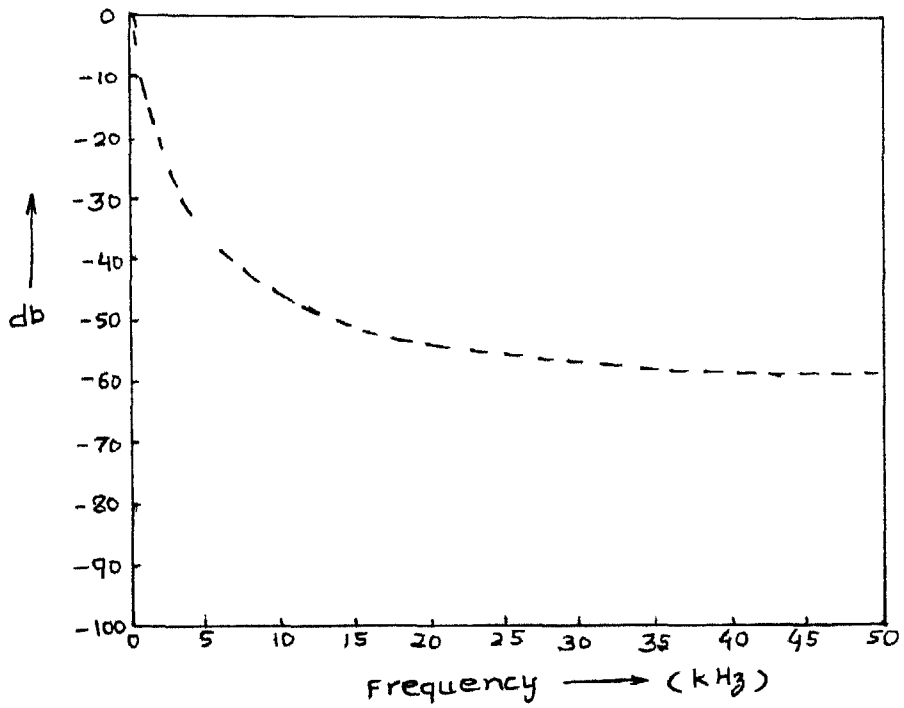

Fig 4 2 A typical envelope of flicker noise spectrum as seen on spectrum analyzer

results are given in Table 4.1(a) and (b).

Table 4.1(a) is for V_{GS} = 3.0 V, and V_{DS} has been varied for bias variation in strong inversion region. As expected, we got almost constant input referred noise within the limitation of experimental accuracy.

Table 4.1(b) corresponds to V_{DS} = 6.0 V, and V_{GS} varied to move the operating point from saturation region to weak inversion region. Measurements at very low drain current were not possible with the present set-up, but the readings given in this table are enough to conclude the following :

1) Input referred noise is independant of current in strong inversion region.
2) As bias is varied from strong inversion to weak inversion region, input noise increases. This behaviour in moderate inversion can not be predicted by eq (4.2) or (4.3), which are for extreme cases. More measurement could not be made in the weak inversion region; but we expect the input noise to go down as V_{GS} is further decreased into weak inversion region, as predicted by eq. (4.3).
3) The same type of behaviour was observed in cross modulation experiment as discussed in the previous chapter. The third order component also assumes a peak in moderate inversion region, and decreases in weak and strong inversion regions.

These results call for the need of modelling in moderate inversion region. We have shown that there exists

TABLE 4.1. Noise Measurement Results.

Input (mV)	Output (mV)	Gain (of MOSFET)	V_{GS} (V)	V_{DS} (V)	Output Noise (RMS) X 2 (mV)	Input Referred RMS Noise (μV)
20	52	2.60	3.08	5.0	20	38
20	69	3.45	3.0	4.5	20	37
20	84	4.20	3.0	4.0	30	35
20	104	5.20	3.0	3.5	35	33
20	120	6.00	3.0	3.0	42	35
20	134	6.70	3.0	2.5	47	35
20	146	7.30	3.0	2.0	55	37
10	80	8.00	3.0	1.5	58	36
10	82	8.20	3.0	1.25	58	35
10	80	8.00	3.0	1.0	55	34
10	70	7.00	3.0	0.75	55	38
10	28.5	2.85	3.0	0.50	26	45

(a)

Input (mV)	Output (mV)	Gain (of MOSFET)	V_{GS} (V)	V_{DS} (V)	Output Noise (RMS) X 2 (mV)	Input Referred RMS Noise (μV)
20	8	0.40	4.00	6.00	4.5	56
20	11	0.55	3.50	6.00	6.0	54
20	16.5	0.825	3.00	6.00	7.0	42
20	21	1.05	2.75	6.00	9.25	44
20	27.5	1.375	2.55	6.00	11	40
20	33.5	1.675	2.40	6.00	14	41
20	40.0	2.0	2.25	6.00	16	40
20	33.5	1.675	2.10	6.00	20	60
20	25	1.25	2.00	5.95	20	80
40	3	0.325	1.85	6.31	5.0	77

(b)

some correlation between the nonlinearity and the noise of MOSFET in weak and moderate inversion regions. This is expected because both of them are influenced by surface state charges. But no correlation exists in linear region as seen in Table 4.1(a). This is because the condition in MOSFET in the linear region is less sensitive to surface states.

Further investigation is needed before anything can be said quantitatively about the correlation between the nonlinearity and noise of the device. Moderate inversion region should be further explored.

CHAPTER V

CONCLUSION

Today's MOSFET models lack the level of precision required for proper analog circuit design. This is specially true of the computationally efficient models used in CAD, which use some approximations that are too crude for some purposes particularly for low voltage applications.

In this present work, MOSFET has been characterized in all the regions of operation using cross modulation technique. It has been shown that subtle nuances of device characteristic can be observed using this technique; third order nonlinearity has been measured experimentally in all the regions of operations. It decreases towards weak inversion region and also towards the satumation region. Thus the importance of device modelling in moderate inversion region is emphasized. A very general model will not serve the purposes of modelling for CAD applications because of its computational complexity. We have suggested a step towards modelling in the moderate inversion region using the general Pao-Sah model. Suitable approximations have to be made in that model to arrive at an analytic equation in the moderate inversion region, thus maintaining a uniformity in transition from weak inversion to strong inversion region.

We have simulated the cross modulation behaviour of MOSFET using SPICE. Parameter extraction for this was done experimentally. Some software has also been developed which is

to be used with SPICE to find the cross modulation components. Comparison of simulated results with the experimental ones has shown large differences although qualitatively they agree.

The present investigation has also shown up a source of nonlinearity even in the linear region. This has been verified for various bias conditions.

The noise behaviour of MOSFET has also been studied. We have measured noise of MOSFET in various regions of operations. It has been proved that flicker noise in moderate inversion can not be predicted by the equations valid in weak inversion and strong inversion regions.

5.1 SUGGESTIONS FOR FURTHER WORK

There exists a lot of scope for further work in precision modelling of MOSFET. We have identified these areas through nonlinearity and noise characterisation. The fact worth mentioning for the measurement and simulation in this characterization is that at every stage proper care has to be taken to avoid extraneous sources of nonlinearity and noise.

We could not probe deep inside the weak inversion region because gain of the system becomes very small and the output signal gets buried in noise. Suitable signal processing can be used for this purpose.

One source of nonlinearity in cross modulation experiment was spectrum analyzer itself. It has to be set properly to avoid any appreciable effect on the measurement

of cross modulation components. For further work some other technique of measurement is suggested. Since only one frequency component is of interest in the output spectrum; a narrow bandpass filtering or frequency shifting can be used.

Theoretical work has to be done in the modelling of device in the moderate inversion region. As mentioned earlier an approximate analytic expression can be found for device operation in this region using the general formulation. To check the validity, the results of that modelling can then be compared with those experimentally obtained by us. The source of nonlinearity in the linear region also needs theoretical modelling.

We did all analysis on NMOS. Nonlinear behaviour of CMOS amplifier can also be investigated. The first order and third order terms are plotted in Fig. 5.1. It shows some asymmetrical behaviour about the characteristic. This may be due to unmatched device (VTO (n-channel) $\simeq$ 1.875 V, VTO (p-channel) $\simeq$ 1.45 V). Through some suitable design technique it should be possible to minimize the nonlinear components.

We used simple oscilloscope method for noise measurement, which is not a very accurate method. Moreover, it averages out all the frequency components of noise. Measurement of spectral density at one particular low frequency would be more meaningful. This can be done by having a small digital system to do sampling

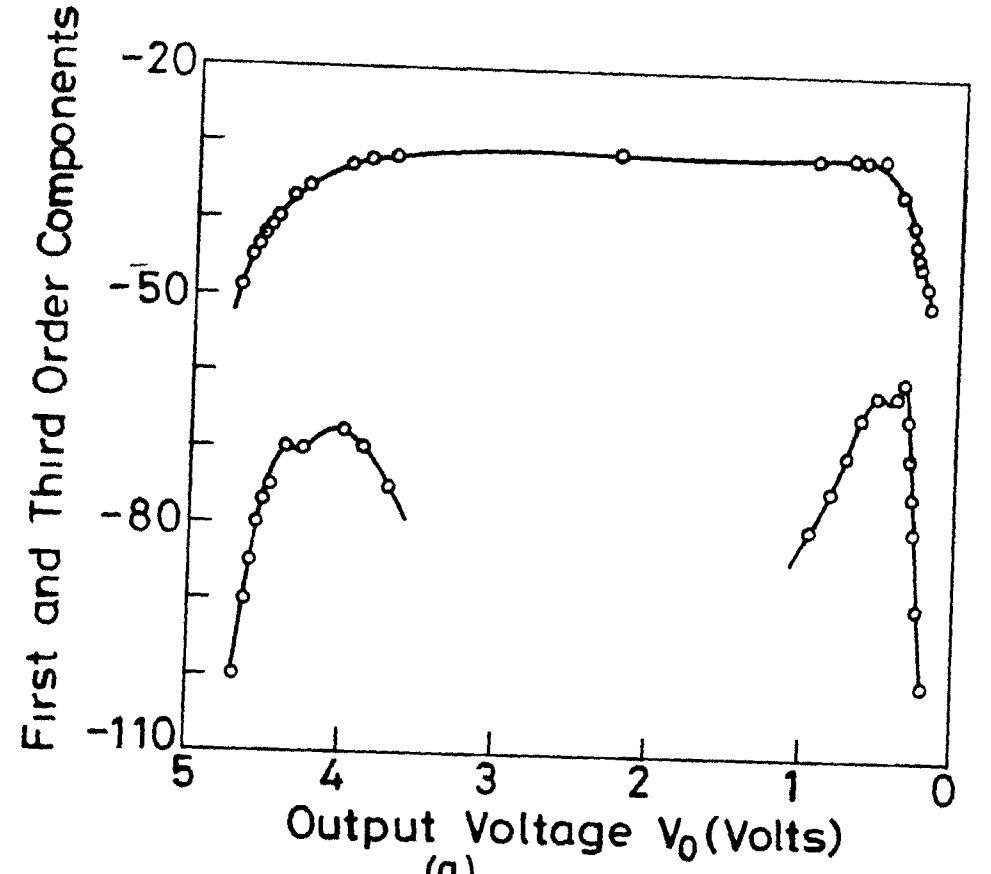

(a)

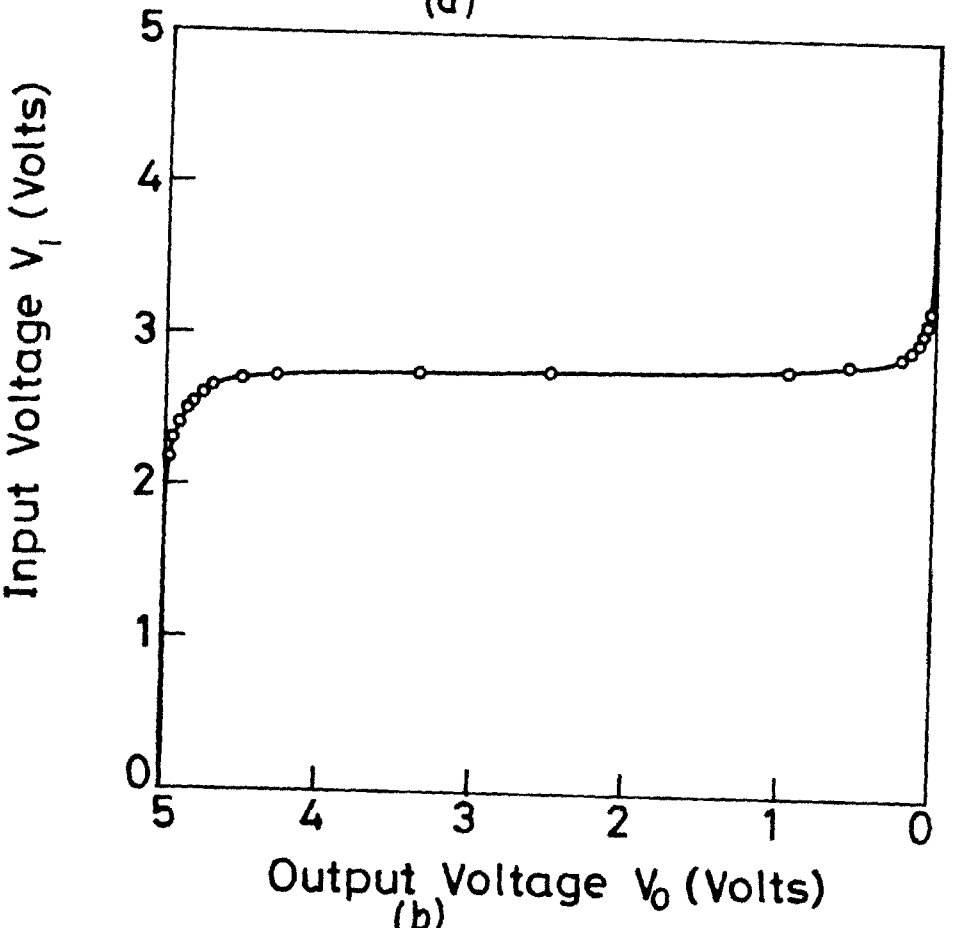

(b)

Fig 5 1 Cross modulation measurement on CMOS
(a) Nonlinear effects vs bias
(b) DC transfer curve

at suitable rate and then taking DFT. Signal analyzers are available to do this job. It can also be done in analog fashion by using a narrow bandpass filter squaring the output signal and then averaging it.

APPENDIX A

TYPES OF NONLINEAR EFFECTS

INTERMODULATION

The process by which two or more signals combine in a nonlinear manner so as to produce new frequency components is termed intermodulation.

CROSS MODULATION

Cross modulation is the nonlinear effect whereby modulation from one signal is transferred to another. In this way severe distortion can be generated by an interferer that is widely separated in frequency from the desired signal.

DESENSITIZATION

The nonlinear effect by which an interfering signal reduces the apparent gain of the system is known as desensitization. For example, if a system is excited by two sinusoidal signals of frequencies f_1 and f_2, from linear considerations the amplitude of the response at f_1 should be unaffected by the presence of the second signal at f_2. However, in actual practice, it is observed that the amplitude of the response at f_1 decreases as the amplitude of the input signal at f_2 exceeds some critical level.

HARMONIC GENERATION

The response of a nonlinear system to a pure sinusoid

is not purely sinusoidal. Due to harmonic generation the output contains sinusoidal components at the fundamental input frequency and its integer multiples.

GAIN COMPRESSION/EXPANSION

For a linear system all the nonlinear transfer functions above order one are identically zero and the voltage gain is a constant equal to the magnitude of the first order transfer function. However the nonlinear transfer functions are not zero in weakly nonlinear system. The voltage gain then depends nonlinearly upon the magnitude of the input signal.

SPURIOUS RESPONSES

The problem of spurious response is one of the primary drawback to the superheterodyne design concept. Spurious responses are defined to be those responses that result from an interfering signal, or one of its harmonics, mixing with the local oscillator signal, or one of its harmonics, to produce a signal that falls within the IF passband.

REFERENCES

[1] Masaki Aoki and Ezaburo Yamada, "Low frequency 1/f noise in MOSFET at low current level," J. Appl. Phy., Vol. 48, pp. 5135-5140, Dec. 1970.

[2] D.M. Miller and R.G. Meyer, "Nonlinearity and cross modulation in FETs," IEEE J. Solid-state Circuits, Vol. SC-6, pp. 244-250, Aug. 1971.

[3] J.S. Vogel, "Nonlinear distortion and mixing processes in FETs," Proc. IEEE, Vol. 55, pp. 2109-2116, Dec. 1967.

[4] R.G. Meyer, M.J. Shensa and R. Eschenbach, "Cross modulation and intermodulation in amplifiers at high frequencies," IEEE J. Solid-state Circuit, Vol. SC-7, pp. 15-23, Feb. 1972.

[5] T.G. Mihran, "A five-parameter model for current and cross modulation in FET with high voltage," IEEE Tran. Electron Devices, Vol. ED-22. pp. 982-988, Nov. 1971.

[6] D.D. Weiner and J.E. Spina, "Sinusoidal Analysis and modelling of weakly Nonlinear Systems," New York : Van Nostrand, 1980.

[7] H.B. Goldberg, "Predict intermodulation distortion from cross modulation measurements," Electron Design, Vol. 18, pp. 76-78, May 10, 1970.

[8] J. Eachus, "Distortion in ultra linear solid-state devices," IEEE J. Solid-state Circuits, Vol. SC-10, pp. 485-497, Dec. 1975.

[9] H.C. Pao and C.T. Sah, ''Effects of diffusion current on characteristics of metal-oxide-(insulator)-semiconductor transistors,'' Solid-state Electron, Vol. 9, pp. 927-937, Oct. 1966.

[10] J.R. Brews, ''A charge sheet model of the MOSFET,'' Solid-state Electron, Vol. 21, pp. 345-355, 1978.

[[1] T. Masuhara, J. Etoh and M. Nagata, ''A precise model for low-voltage circuits,'' IEEE Trans. Electron Devices, Vol. ED-21, pp. 363-371, June 1974.

[12] Y Tsividis, ''Problems in precision modelling of the MOS transistor for analog applications,'' IEEE Tran. CAD, Vol. CAD-3, pp. 72-79, Jan. 1984.

[13] Y. Tsividis, ''Moderate inversion in MOS devices,'' Solid-state Electron, Vol. 26, pp. 1099-1104, 1982.

[14] D. Lieberman, ''Cross modulation figure of merit for transistor amplifier stages,'' Proc. IEEE, Vol. 58, pp. 1063-1071, July, 1970.

[15] R.M. Swanson and J.D. Meindl, ''Ion-implemented complementory MOS transistors in low-voltage circuits,'' IEEE J. Solid-state Circuits, Vol. SC-7, pp. 146-153, Apr. 1972.

[16] A. Antoniou, ''Digital Filter Analysis and Design,'' New Delhi Tata McGraw Hill, 1980.

[17] G. Reimbold, ''Modified 1/f trapping noise theory and experiments in MOS transistors biased from weak inversion to strong inversion,'' IEEE Trans. Electron Device, Vol. ED-31, Sept. 1984.

[18] G.M. Miller, ''Modern Electronic Communication,'' Englewood Cliffs, NJ : Prentice-Hall, 1978.